Title

Cognitive impairment and transcriptomic profile in hippocampus of young mice after multiple neonatal exposures to sevoflurane

Journal

Aging, 11(19)

ISSN

1945-4589

Authors

Song, Shao-Yong
Meng, Xiao-Wen
Xia, ZhengYuan
et al.

Publication Date

2019-10-03

DOI

10.18632/aging.102326

Peer reviewed

Research Paper

Cognitive impairment and transcriptomic profile in hippocampus of young mice after multiple neonatal exposures to sevoflurane

Shao-Yong Song[1,*], Xiao-Wen Meng[1,*], ZhengYuan Xia[2,3], Hong Liu[3], Juan Zhang[1], Qing-Cai Chen[1], Hua-Yue Liu[1], Fu-Hai Ji[1], Ke Peng[1]

[1]Department of Anesthesiology, First Affiliated Hospital of Soochow University, Suzhou, Jiangsu, China
[2]Department of Anesthesiology, University of Hong Kong, Hong Kong, China
[3]Department of Anesthesiology and Pain Medicine, University of California Davis Health System, Sacramento, CA 95817, USA
*Equal contribution

Correspondence to: Fu-Hai Ji, Ke Peng; **email:** jifuhaisuda@163.com, pengke0422@163.com
Keywords: sevoflurane, cognitive function, hippocampus, RNA sequencing, differentially expressed genes
Received: June 15, 2019 **Accepted:** September 22, 2019 **Published:** October 3, 2019

ABSTRACT

Children with repeated inhalational anesthesia may develop cognitive disorders. This study aimed to investigate the transcriptome-wide response of hippocampus in young mice that had been exposed to multiple sevoflurane in the neonatal period. Mice received 3% sevoflurane for 2 h on postnatal day (PND) 6, 8, and 10, followed by arterial blood gas test on PND 10, behavioral experiments on PND 31–36, and RNA sequencing (RNA-seq) of hippocampus on PND 37. Functional annotation and protein-protein interaction analyses of differentially expressed genes (DEGs) and quantitative reverse transcription polymerase chain reaction (qPCR) were performed. Neonatal sevoflurane exposures induced cognitive and social behavior disorders in young mice. RNA-seq identified a total of 314 DEGs. Several enriched biological processes (ion channels, brain development, learning, and memory) and signaling pathways (oxytocin signaling pathway and glutamatergic, cholinergic, and GABAergic synapses) were highlighted. As hub-proteins, Pten was involved in nervous system development, synapse assembly, learning, memory, and behaviors, Nos3 and Pik3cd in oxytocin signaling pathway, and Cdk16 in exocytosis and phosphorylation. Some top DEGs were validated by qPCR. This study revealed a transcriptome-wide profile in mice hippocampus after multiple neonatal exposures to sevoflurane, promoting better understanding of underlying mechanisms and investigation of preventive strategies.

INTRODUCTION

In a recent epidemiologic study of 20,922 children in the US, approximately 1 in 7 children experienced at least 1 episode of surgical procedure under general anesthesia before 3 years of age [1]. Of them, more than 1 in 4 children who received general anesthesia were at high risk for neurodevelopmental problems, as defined by Food and Drug Administration warning—"repeated or lengthy use of general anesthetic and sedative agents may affect brain development in children < 3 years" [1, 2].

Over the years, studies have shown that anesthesia and surgery during childhood was associated not only with postoperative behavioral changes, but also with long-term deficits in neurocognitive function, learning ability, and academic performance [3–7]. Recent studies provided evidence that a single brief anesthesia for approximately 1 h in infancy or under age 3 did not have significant impact on neurodevelopment [8–10]; however, in children receiving multiple anesthesia exposures, their parents reported problems of behaviors, executive function, and reading [11]. Animal studies also indicated neurotoxicity after neonatal exposure to

general anesthesia [12–17]. To date, the extent of the risk of neurotoxicity associated with anesthetics and the exact mechanisms remain elusive.

Sevoflurane is the most popular inhalational anesthetic agent for pediatric patients, with excellent properties of respiratory tolerance, rapid onset, rapid offset, and hemodynamic stability [18]. Recent studies showed that repeated sevoflurane exposures in the neonatal period led to subsequent learning impairment, memory deficits, and behavioral abnormalities in the young animal [12, 19–21]. However, these studies investigated the expression of several genes, related proteins, and a small number of signaling pathways.

Several brain regions including hippocampus, parahippocampal cortex, entorhinal cortex, retrosplenial cortex, and dorsolateral prefrontal cortex are involved in the cognitive processes [22, 23]. Of these, the hippocampus plays an essential role in navigation, cognition, and memory. Animal studies showed that gene knockout or pharmacological intervention in the hippocampus caused loss of learning ability and memory storage [24, 25]. In addition, the hippocampus and prefrontal cortex are related to impairments in cognitive function and memory during aging [26, 27].

In this study, the model of multiple neonatal exposures to sevoflurane was used to assess cognitive function, social interaction, anxiety, depression, and stereotyped behaviors in young mice. The main objective was to reveal the genome-wide expression profile and differentially expressed genes (DEGs) in the hippocampus between sevoflurane-treated and control mice by using the high-throughput mRNA-sequencing (RNA-seq). The biological processes, signaling pathways, and protein interactions of target DEGs were analyzed. Furthermore, real-time quantitative reverse transcription polymerase chain reaction (qPCR) assays were performed to validate the RNA-seq results.

RESULTS

Multiple neonatal exposures to sevoflurane led to cognitive and social behavior impairment in the young mice

The study design is presented in Figure 1A. After sevoflurane anesthesia on postnatal day (PND) 6, 8, and 10, arterial blood gas tests were performed on PND 10, behavioral tests were carried out on PND 31–36, and the hippocampal tissues were harvested on PND 37 for RNA-Seq analysis.

Cognitive function was evaluated using the Morris water maze (MWM) test. In the testing phase on PND 36, mice in the sevoflurane group had longer mean distance from the platform (0.33 ± 0.02 vs. 0.26 ± 0.01 m, $p = 0.006$) and fewer platform-crossing times (2.20 ± 0.55 vs. 4.60 ± 0.65, $p = 0.011$) compared to the control group (Figure 1B), while time spent in the fourth quadrant did not differ between the two groups. In the training phase on PND 32–35, the sevoflurane group showed longer escape latency than the control group (31.36 ± 2.37 vs. 13.91 ± 1.44 s, $p < 0.0001$ for PND 34; Figure 1C).

In addition, social interaction tests were carried out. In the habituation session, both groups spent similar time sniffing at the left and right empty enclosures (Figure 1D). In the sociability session, both groups spent more time sniffing at Stranger 1 than at the empty enclosure (Figure 1E). In the preference for social novelty session, the control group spent more time sniffing at Stranger 2 than Stranger 1 (81.05 ± 6.60 vs. 42.31 ± 5.64 s, $p = 0.02$; Figure 1F), while the sevoflurane group showed no difference (80.48 ± 15.53 vs. 64.73 ± 7.57 s, $p = 0.48$).

Multiple neonatal exposures to sevoflurane did not induce anxiety-like, depression-like, or stereotyped behaviors

First, in the open field test, two groups had similar time of stay in the center, speed of movement, and distance traveled (Supplementary Figure 1A–1C), indicating that sevoflurane did not induce anxiety-like behaviors. Next, in the elevated plus maze and light-dark box tests, the two groups had similar time in the open arms, numbers of open and closed arms entries, and time in the caliginous section (Supplementary Figure 1D–1G), suggesting no significant depression-like behaviors. Finally, in the self-grooming test, similar numbers and time of self-grooming showed that sevoflurane did not induce stereotyped behaviors (Supplementary Figure 1H–1I).

Oxygenation and homeostasis were maintained during sevoflurane anesthesia

To rule out the possibility that the specific changes noted in behaviors or gene expression may be due to poor oxygenation, arterial blood samples were taken for analysis at PND 10 in the sevoflurane group. The value of PO_2 was lower at 115 min than that at 5 min (89.25 ± 1.66 vs. 94.13 ± 0.91 mmHg, $p = 0.02$; Supplementary Figure 2A), but both within the normal range. In addition, the other parameters including PCO_2, Hct, pH, Na^+, K^+, Ca^+, and Cl^- remained stable (Supplementary Figure 2B–2H).

RNA-seq analysis identified 49 up-regulated and 265 down-regulated DEGs

RNA-seq analysis showed the expression level of 17,107 genes in the mice hippocampus of the sevoflurane and

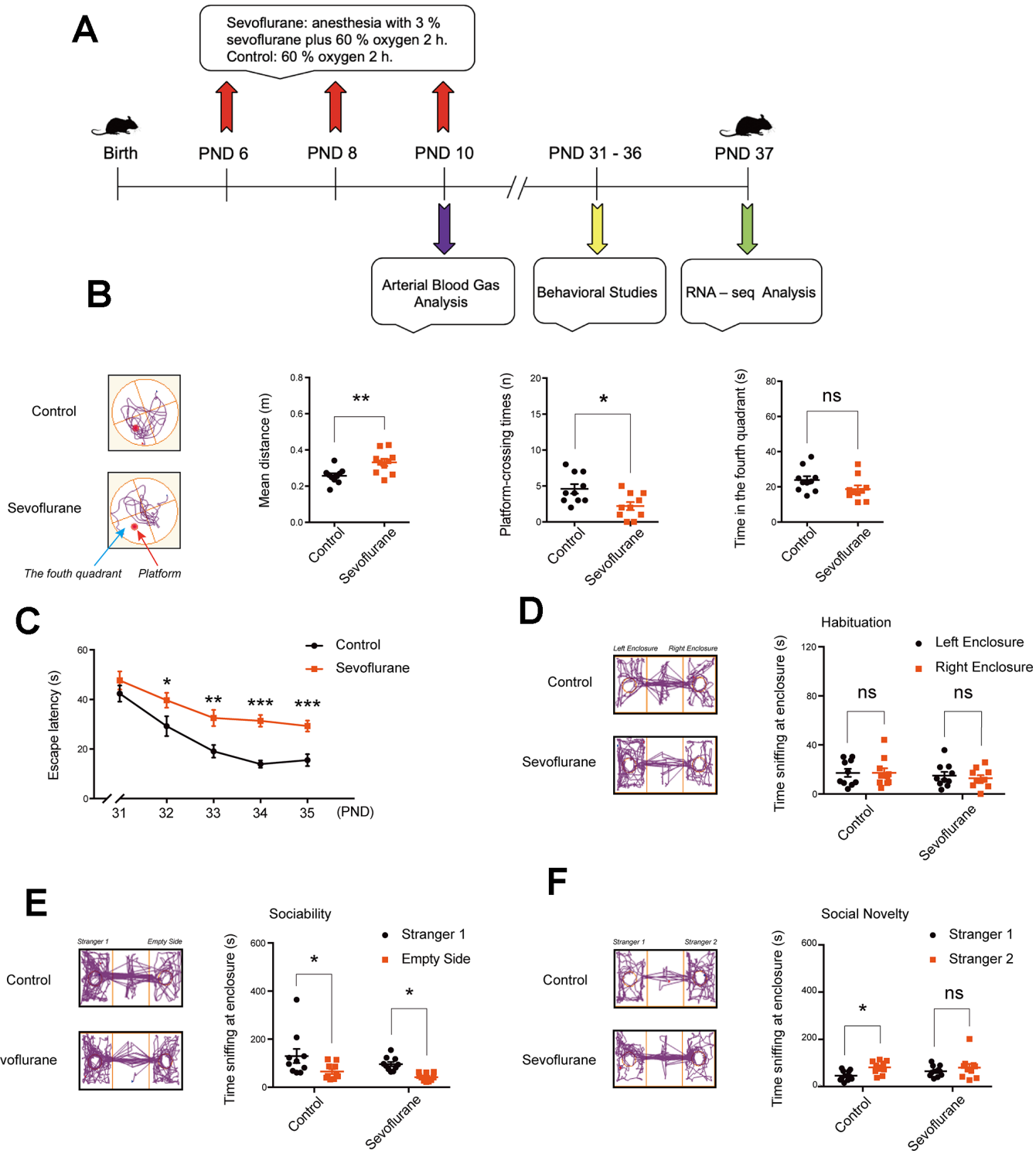

Figure 1. Cognitive function and social behaviors in young mice after multiple sevoflurane exposures during the neonatal period. (**A**) 3% sevoflurane 2 h daily on postnatal day (PND) 6, 8, and 10, arterial blood test on PND 10, behavioral test on PND 31–36, and RNA-seq analysis of hippocampal tissues on PND 37. (**B**) Morris water maze (testing phase on PND 36) showing longer mean distance from the original platform area and fewer platform-crossing times in the sevoflurane group, without significant difference in time spent in the fourth quadrant. (**C**) Morris water maze (training phase on PND 31–35) showing longer escape latency in the sevoflurane group. (**D**) Social interaction test on habituation showing no significant difference in time of sniffing at the left and right empty enclosures for both groups. (**E**) Social interaction test on sociability showing that both groups spent more time sniffing at Stranger 1 than at the empty enclosure. (**F**) Social interaction test on preference for social novelty showing that the control group, but not sevoflurane group, spent more time sniffing at Stranger 2 than Stranger 1. n = 10. *$p < 0.05$, **$p < 0.01$, ***$p < 0.001$ for the comparisons shown.

control groups. Of these, a total of 314 DEGs were determined (Figure 2A), including 49 up-regulated genes (Figure 2B, Supplementary Table 2) and 265 down-regulated genes (Figure 2C, Supplementary Table 3). These DEGs present differential expression profiles, which distinguishes the sevoflurane group from the control group apparently. The top 20 up- and down-regulated DEGs are listed in Table 1.

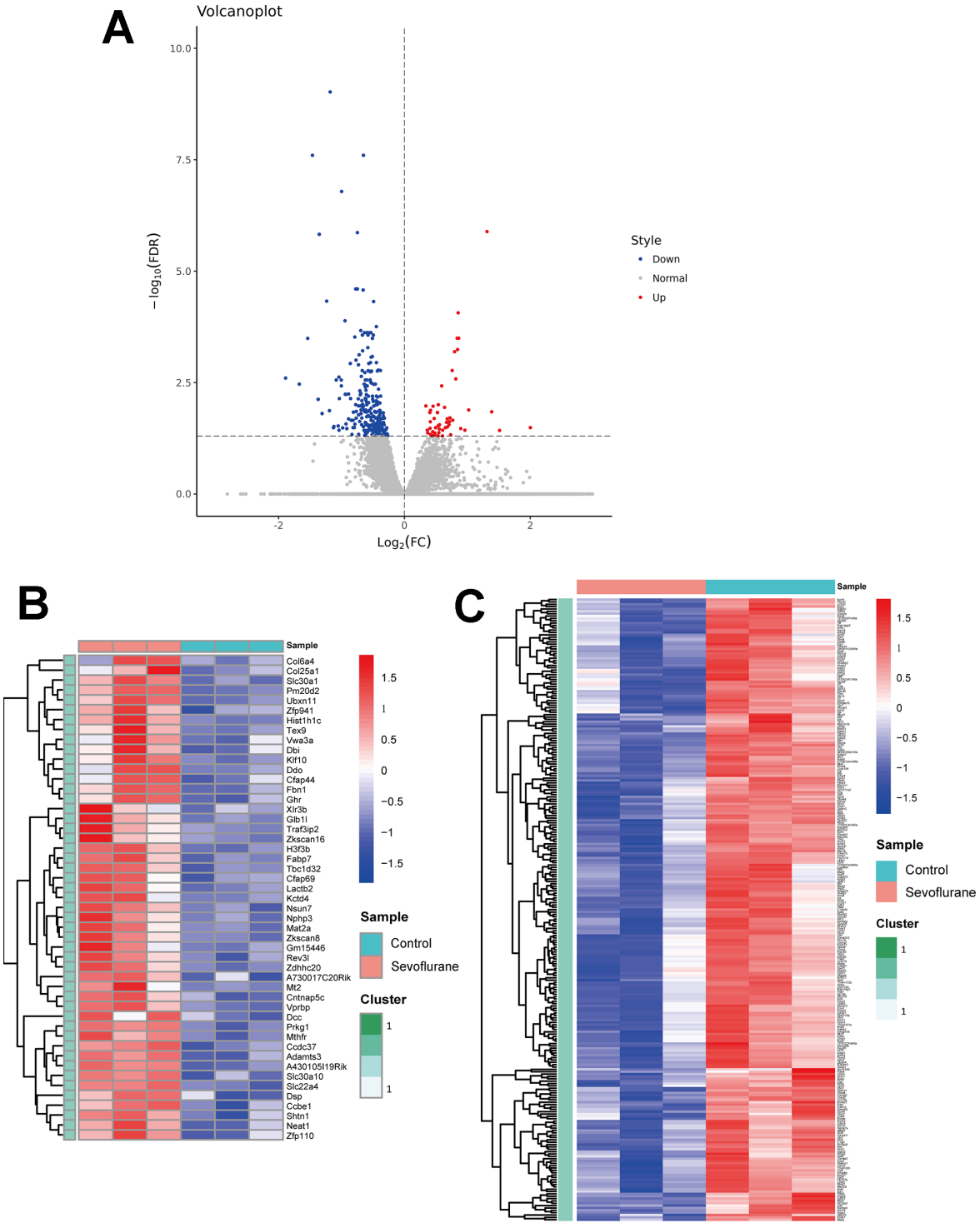

Figure 2. Volcano plot and heatmaps of DEGs in hippocampal tissues between sevoflurane-treated and control mice. (**A**) Volcano plot showing up-regulated (red dots) and down-regulated (blue dots) DEGs and normally expressed genes (gray dots). (**B**) Heatmap of 49 up-regulated DEGs. (**C**) Heatmap of 265 down-regulated DEGs.

Table 1. Top 20 up-regulated and down-regulated DEGs.

Gene	log_2FC	*p*-value	FDR	Location
Up-regulated				
Hist1h1c	1.312676	5.32E-10	1.29E-06	chr13:23738807-23739531
Fabp7	0.853611	9.19E-08	8.57E-05	chr10:57784923-57788450
Neat1	0.836954	6.96E-07	0.000319	chr19:5824710-5845478
Tbc1d32	0.862511	7.10E-07	0.000319	chr10:56014294-56228689
Klf10	0.843942	1.46E-06	0.000573	chr15:38294406-38300711
Mt2	0.796616	1.74E-06	0.00064	chr8:94172618-94173567
Fbn1	0.758222	6.25E-06	0.001693	chr2:125300594-125506438
Ccbe1	0.815541	1.23E-05	0.002613	chr18:66056856-66291838
Prkg1	0.591146	2.20E-05	0.003748	chr19:30564487-31765033
Pm20d2	0.537705	9.04E-05	0.009937	chr4:33170406-33189737
H3f3b	0.34208	0.000102	0.01057	chr11:116021961-116024504
Slc30a1	0.456209	0.000105	0.010728	chr1:191906781-191913247
Cntnap5c	0.637167	0.000114	0.011397	chr17:57769570-58410342
Ddo	1.020954	0.000134	0.01302	chr10:40630011-40649931
Mthfr	0.416183	0.000141	0.013283	chr4:148041189-148059562
Cfap44	1.387494	0.000160	0.014272	chr16:44394799-44482428
Mat2a	0.40471	0.000174	0.014828	chr6:72432799-72439558
Zkscan8	0.524755	0.000175	0.014828	chr13:21513221-21531114
Cfap69	0.72325	0.000263	0.019481	chr5:5580982-5664232
Slc30a10	0.474247	0.000284	0.020126	chr1:185454848-185468761
Down-regulated				
Sdf2l1	-1.1809	7.82E-14	9.48E-10	chr16:17130138-17132383
E130012A19Rik	-1.4612	5.89E-12	2.51E-08	chr11:97627387-97629716
Gatsl2	-0.65162	6.22E-12	2.51E-08	chr5:134099748-134141758
Rims4	-0.99919	5.35E-11	1.62E-07	chr2:163863881-163918683
Doc2a	-0.74835	6.73E-10	1.36E-06	chr7:126847553-126852705
Klf4	-1.35382	8.59E-10	1.49E-06	chr4:55527137-55532475
Efhd2	-0.74812	1.74E-08	2.51E-05	chr4:141858142-141874920
Ccdc184	-0.7742	1.86E-08	2.51E-05	chr15:98167806-98170134
Stx1a	-0.65659	2.18E-08	2.65E-05	chr5:135023572-135051099
Sox18	-1.23674	4.24E-08	4.68E-05	chr2:181669837-181671640
Nr2f1	-0.49017	4.73E-08	4.78E-05	chr13:78188973-78198982
Cit	-0.94487	1.49E-07	0.000129	chr5:115845656-116006341
9430020K01Rik	-0.44648	2.16E-07	0.000175	chr18:4634929-4682869
Kcnab3	-0.69399	2.83E-07	0.000215	chr11:69326258-69333041
Lasp1	-0.63517	3.35E-07	0.000239	chr11:97799672-97838764
Cacna1i	-0.53254	3.60E-07	0.000239	chr15:80287238-80398292
Fosl2	-0.59154	3.75E-07	0.000239	chr5:32136472-32157839
Pdia6	-0.55648	3.98E-07	0.000239	chr12:17266595-17284770
Xbp1	-0.59461	4.14E-07	0.000239	chr11:5520641-5525993
Pgr	-0.5794	5.15E-07	0.000271	chr9:8899833-8968611

DEG, differentially expressed gene; FDR, false discovery rate.

Gene Ontology (GO) analysis revealed significantly enriched GO terms and interactions of biological processes

For the biological process, the top 10 categories with associated DEGs are presented in Table 2. The top 3 enriched GO terms of up-regulated DEGs were positive regulation of vascular endothelial growth factor signaling pathway, cellular zinc ion homeostasis, and zinc ion transport (Figure 3A), while those associated with down-regulated DEGs included regulation of ion transmembrane transport, potassium ion transmembrane transport, and potassium ion transport (Figure 3B). Several significantly enriched biological processes were related to brain development (nervous system development, exocytosis, synapse assembly, and phosphorylation) and cognitive function (learning, memory, and long-term memory), all of which were associated with down-regulated DEGs. All GO terms of biological process are listed in Supplementary Tables 4–5.

The enriched GO terms of DEGs were also classified according to cellular component and molecular function. For cellular component, the most significantly categories were collagen trimer for up-regulated DEGs (Figure 3C) and synapse for down-regulated DEGs (Figure 3D). All GO terms on cellular component are shown in Supplementary Tables 6–7. For molecular function, the most significantly categories were cation transmembrane transporter activity for up-regulated DEGs (Figure 3E) and voltage-gated ion channel activity for down-regulated DEGs (Figure 3F). All GO terms on molecular function are shown in Supplementary Tables 8–9.

GO-Tree analysis illustrated the interactions within the biological processes, as shown in Figure 4. A total of 37 GO terms were involved, with 5 terms associated with up-regulated genes and 32 terms associated with down-regulated genes (Supplementary Table 10). There were several types of relations including complete subordination, partly subordination, positive regulation, and negative regulation within the GO terms.

Pathway analysis revealed significantly enriched signaling pathways and their relationship

Kyoto Encyclopedia of Genes and Genomes (KEGG) pathway analysis revealed 40 significantly enriched signaling pathways, including 3 associated with up-regulated DEGs and 37 associated with down-regulated DEGs. The top enriched pathways for up- and down-regulated genes are presented in Table 3. Mineral absorption, PPAR signaling pathway, and one carbon pool by folate were the top 3 enriched pathways associated with up-regulated DEGs (Figure 5A). For down-regulated DEGs, the top 3 enriched pathways were oxytocin signaling pathway, protein processing in endoplasmic reticulum, and glutamatergic synapse (Figure 5B). Several significantly enriched signaling pathways were associated with the regulation of synapses, including glutamatergic synapse, cholinergic synapse, and GABAergic synapse. All results of KEGG pathway enrichment are listed in Supplementary Tables 11–12.

Pathway network analysis showed the upstream and downstream relationship of the significantly enriched signaling pathways (Figure 5C). A total of 30 signaling pathways were involved, all of which were associated with down-regulated DEGs. (Supplementary Table 13). Calcium signaling pathway, synaptic vesicle cycle, and GABAergic synapse were the top 3 pathways with rich connections with other pathways.

GO and KEGG pathway analysis of top 20 up- and down-regulated DEGs

To further investigate the role of top 20 up- and down-regulated DEGs, GO and KEGG analyses were carried out. These genes were labeled in the volcano plot (Supplementary Figure 3A), and their differential expression profiles were visualized in heatmaps (Supplementary Figure 3B–3C). Based on these DEGs, significantly enriched biological processes, cellular components, and molecular functions were categorized by GO analysis (Supplementary Figure 3D–3E). Besides, KEGG pathway analysis found several significantly enriched pathways associated with up- and down-regulated DEGs (Supplementary Figure 3F–3G).

Protein-protein interaction (PPI) network revealed several hub proteins

PPI network analysis showed the interactions among the proteins. Several hub proteins that had rich connectivity with other proteins were identified. Pten (degree = 16), Nos3 (degree = 14), Pik3cd (degree = 12), Cdk16 (degree = 11), Rhobtb2 (degree = 11), Hyou1 (degree = 9), Hspa5 (degree = 9), Pdia4 (degree = 8), Pdia6 (degree = 8), Tbr1 (degree = 8) were the top 10 hub proteins (Figure 6). All results of protein-protein interactions are shown in Supplementary Figure 4.

RNA-Seq results were validated by qPCR

The top 20 up- and down-regulated DEGs from RNA-seq analysis were verified by qPCR. For up-regulated DEGs, both RNA-seq analysis and qPCR revealed 9 genes with significantly positive expression change (*Fabp7*, *Klf10*, *Mt2*, *Ccbe1*, *Slc30a1*, *Mthfr*, *Cfap44*, *Zkscan8*, and *Cfap69*), while the expression of *Prkg1*

Table 2. Top 10 enriched BP terms of up-regulated and down-regulated DEGs.

ID	Term	DEG(s)	*p*-value	FDR	Enrichment
Up-regulated					
GO:1900748	positive regulation of vascular endothelial growth factor signaling pathway	*Adamts3, Ccbe1*	1.503E-05	0.0040579	294.52778
GO:0006882	cellular zinc ion homeostasis	*Slc30a1, Mt2*	0.0003851	0.0406079	67.967949
GO:0006829	zinc ion transport	*Slc30a1, Slc30a10*	0.0015749	0.0406079	33.983974
GO:0006730	one-carbon metabolic process	*Mat2a, Mthfr*	0.0020959	0.0406079	29.452778
GO:0035212	cell competition in a multicellular organism	*Vprbp*	0.0022635	0.0406079	441.79167
GO:0090230	regulation of centromere complex assembly	*H3f3b*	0.0022635	0.0406079	441.79167
GO:0030575	nuclear body organization	*Neat1*	0.0022635	0.0406079	441.79167
GO:1990245	histone H2A-T120 phosphorylation	*Vprbp*	0.0022635	0.0406079	441.79167
GO:0036018	cellular response to erythropoietin	*Mt2*	0.0022635	0.0406079	441.79167
GO:0071584	negative regulation of zinc ion transmembrane import	*Slc30a1*	0.0022635	0.0406079	441.79167
Down-regulated					
GO:0034765	regulation of ion transmembrane transport	*Cacng2, Kcnh3, Kcna3, Kcnj4, Cacna1i, Kcnc4, Kcnab3, Kcnj11, Scn1b, Kcnj9, Kcnf1, Kcnb1, Cacng7, Kcnk3, Kcnc1, Kcnj2*	6.587E-10	8.642E-07	7.3469317
GO:0071805	potassium ion transmembrane transport	*Kcnh3, Kcna3, Kcnk12, Kcnj4, Kcnc4, Kcnab3, Kcnj11, Kcnf1, Kcnb1, Kcnk3, Kcnc1, Kcnj2*	6.591E-08	3.715E-05	7.5871199
GO:0006813	potassium ion transport	*Kcnh3, Kcna3, Kcnj4, Kcnc4, Kcnab3, Kcnj11, Kcnj9, Kcnf1, Kcnb1, Kcnk3, Kcnc1, Kcnj2*	8.495E-08	3.715E-05	7.4159818
GO:0000122	negative regulation of transcription from RNA polymerase II promoter	*Scrt1, Fgfr3, Mxi1, Egr1, Pou3f3, Zbtb16, Nfix, Bcl6, Nr2f1, Klf5, Tbx3, Eng, Xbp1, Fezf2, Satb2, Calr, Dab2ip, Ppard, Foxg1, Sox18, Hivep1, Dusp26, Klf4, Cry1*	4.431E-06	0.0014534	2.850652
GO:0007399	nervous system development	*Igsf9, Ina, Pou3f3, Sema7a, Nes, Nr2f1, Lmtk2, Fezf2, Cit, Ndel1, Brsk1, Nrsn1, Gdpd5, Sema6c, Bax, Pten*	8.858E-06	0.0023242	3.6734659
GO:0018105	peptidyl-serine phosphorylation	*Ulk1, Adrbk1, Pink1, Lmtk2, Brsk1, Ttbk1, Csnk1e, Sbk1*	1.945E-05	0.0041297	6.9952169
GO:0006811	ion transport	*Cacng2, Kcnh3, Kcna3, Slc38a2, Kcnk12, Kcnj4, Cacna1i, Lasp1, Kcnc4, Fxyd7, Kcnab3, Kcnj11, Grid1, Scn1b, Kcnj9, Kcnf1, Kcnb1, Cacng7, Kcnk3, Kcnc1, Kcnj2*	2.203E-05	0.0041297	2.8111885
GO:0006887	exocytosis	*Stxbp1, Doc2a, Cdk16, Stx1a, Rims3, Srcin1, Rims4, Cplx1*	3.524E-05	0.0057795	6.4465724
GO:0007416	synapse assembly	*Plxnd1, Farp1, Shank2, Clstn3, Pten Camk2n2, Prkar1b, Fgfr3, Ulk1,*	4.606E-05	0.0067145	12.453606
GO:0016310	phosphorylation	*Limk1, Adrbk1, Cdk16, Pink1, Lmtk2, Stk32c, Nlk, Cit, Brsk1, Pik3cd, Ttbk1, Pak6, Camkk2, Tnk2, Mast2, Csnk1e, Sbk1, Cerk*	5.219E-05	0.0068479	2.575874

BP: biological process; DEG: differentially expressed gene; FDR: false discovery rate.

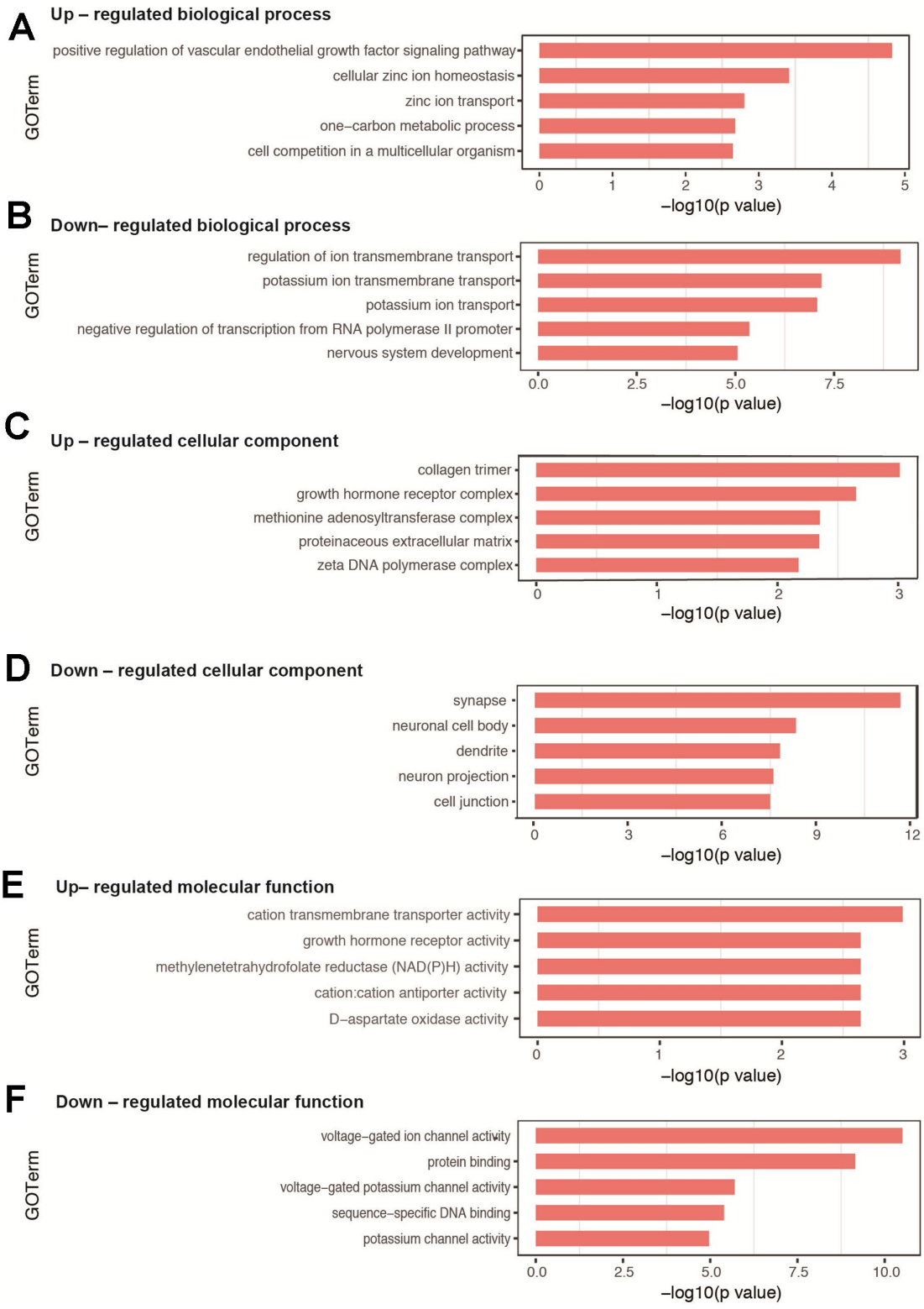

Figure 3. GO analysis of DEGs in hippocampal tissues between sevoflurane-treated and control mice. (**A**, **B**) Top 5 GO terms of biological process based on up- and down-regulated DEGs. (**C**, **D**) Top 5 GO terms of cellular component based on up- and down-regulated DEGs. (**E**, **F**) Top 5 GO terms of molecular function based on up- and down-regulated DEGs. Blue columns indicate terms without significant difference.

showed a negative change in the qPCR results (Figure 7). For down-regulated DEGs, both methods identified 9 genes with a significantly negative expression change (*Sdf2l1*, *Gatsl2*, *Klf4*, *Sox18*, *Nr2fl*, *Cacna1i*, *Fols2*, *Pdia6*, and *Xbp1*), while qPCR showed that the expression of *Ccdc184* changed positively (Figure 8).

DISCUSSION

This is the first study revealing the genome-wide response of the transcriptome of the hippocampus of young mice to neonatal sevoflurane exposures for 3 non-consecutive days. Sevoflurane induced cognitive impairment and social behavior disorders in young mice, but not anxiety-like, depression-like, or stereotyped behaviors. During the sevoflurane procedures, oxygenation and homeostasis were maintained. RNA-seq analysis of the hippocampal tissues identified a total of 314 DEGs and revealed their functional enrichment and interactions. The most significantly enriched biological processes included positive regulation of vascular endothelial growth factor signaling pathway and regulation of ion transmembrane transport. The most significantly enriched signaling pathways included mineral absorption and oxytocin signaling pathway. Pten, Nos3, and Pik3cd were the top 3 hub proteins. The expression of some top DEGs were confirmed by qPCR.

During the human brain development, a unique peak of synaptogenesis occurs in the primary sensorimotor cortex near the birth, temporal cortex at 9 months, and

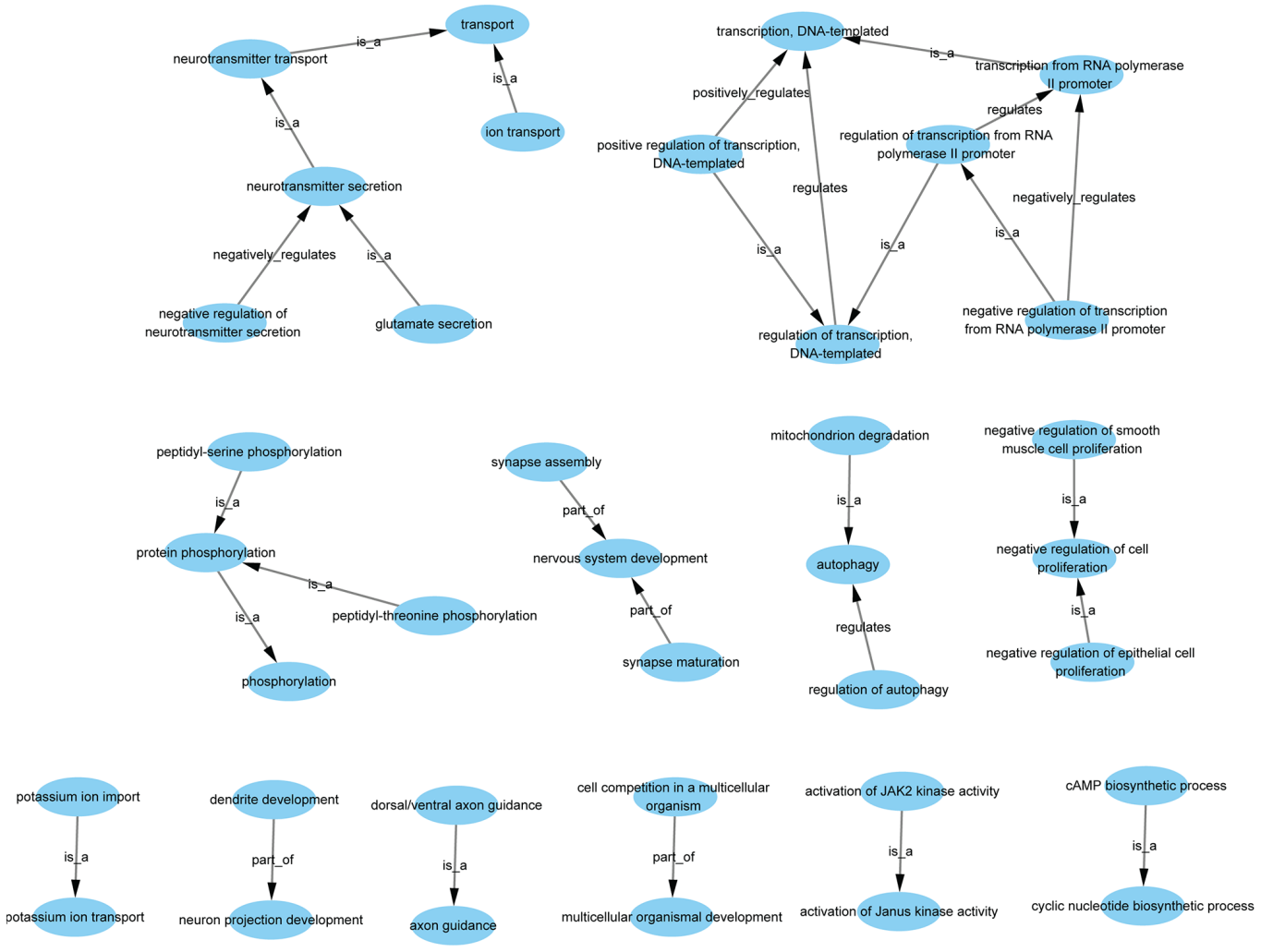

Figure 4. GO-tree analysis based on biological process. Arrow source, a GO term at a lower level; arrow target, a GO term at a higher level. Relation: is a, the downstream GO term is completely subordinate to the upstream GO term; part of, a part of the downstream GO term is subordinate to the upstream GO term; regulates, the downstream GO term can regulate the upstream GO term; positive regulates, the downstream GO term can regulate the upstream GO term positively; negative regulates, the downstream GO term can regulate the upstream GO term negatively.

Table 3. Signaling pathway enrichment of up-regulated and down-regulated DEGs.

ID	Term	DEG(s)	*p*-value	FDR	Enrichment
Up-regulated					
PATH:04978	Mineral absorption	*Slc30a1, Mt2*	0.0037153	0.1263212	21.611594
PATH:03320	PPAR signaling pathway	*Dbi, Fabp7*	0.0111679	0.1898536	12.273251
PATH:00670	One carbon pool by folate	*Mthfr*	0.0375845	0.3333577	26.161404
Down-regulated					
PATH:04921	Oxytocin signaling pathway	*Cacng2, Adcy1, Kcnj4, Kcnj9, Adcy8, Pik3cd, Elk1, Adcy4, Camkk2, Cacng7, Nos3, Kcnj2*	2.428E-07	3.569E-05	6.5089481
PATH:04141	Protein processing in endoplasmic reticulum	*Ubqln4, Hspa5, Hyou1, Syvn1, Xbp1, Calr, Pdia4, Fbxo2, Pdia6, Bax, Man1c1*	2.924E-06	0.0002149	5.71341
PATH:04724	Glutamatergic synapse	*Slc38a2, Grm4, Adcy1, Grm2, Adrbk1, Glul, Adcy8, Adcy4, Shank2*	1.52E-05	0.000745	6.0733098
PATH:04915	Estrogen signaling pathway	*Adcy1, Kcnj9, Adcy8, Pik3cd, Fkbp4, Adcy4, Nos3*	0.0001353	0.0049722	6.1215107
PATH:04971	Gastric acid secretion	*Adcy1, Sst, Adcy8, Cckbr, Adcy4, Kcnj2*	0.0002082	0.0061217	6.9487418
PATH:04261	Adrenergic signaling in cardiomyocytes	*Cacng2, Adrb1, Adcy1, Scn1b, Adcy8, Pik3cd, Adcy4, Cacng7*	0.0003244	0.0079469	4.601404
PATH:05414	Dilated cardiomyopathy	*Cacng2, Adrb1, Adcy1, Adcy8, Adcy4, Cacng7*	0.0005682	0.0119312	5.7776056
PATH:05020	Prion diseases	*Egr1, Hspa5, Elk1, Bax*	0.0006871	0.0126259	9.7944171
PATH:04918	Thyroid hormone synthesis	*Adcy1, Hspa5, Adcy8, Pdia4, Adcy4*	0.0013702	0.0223796	6.0352922
PATH:04725	Cholinergic synapse	*Adcy1, Kcnj4, Adcy8, Pik3cd, Adcy4, Kcnj2*	0.0018898	0.0277797	4.591133

DEG: differentially expressed gene; FDR: false discovery rate.

prefrontal cortex at age 3, which is also known as a window of vulnerability [28]. For rodents, the vulnerability window seems to happen on PND 7–30 when exposure to sevoflurane affected brain development [14, 29, 30]. In terms of the sevoflurane concentration, our study used a clinically relevant anesthetic concentration (minimum alveolar concentration of 3.3 ± 0.2% in human neonates) [31]. In addition, studies suggest that 3% sevoflurane did not significantly alter the values of pH, arterial oxygen tension, arterial carbon dioxide tension, or electrolyte contents in mice [31, 32], which was in line with our blood gas results. Thus, the anesthesia protocol of 3% sevoflurane for 2 h on PND 6, 8, and 10 was used in this study. Regarding the MWM test, mice at one-month age may experience relative higher stress in the Morris water maze as compared to adult mice. In fact, MWM performance may be affected by several factors including training procedure, apparatus, and characteristics of the experimental animals (species, strain, sex, age, nutritional status, stress, and infection) [33]. The MWM test has been successfully used to determine cognitive function in young mice at 1-month age in recent studies [12, 20].

Studies showed that neonatal sevoflurane exposures induced long-term neurodegenerative change, learning disability, and memory impairment [12, 34–37]. In the immature brain, sevoflurane caused excitatory effects of the type A gamma-amino butyric acid (GABA-A) receptors, which might contribute to sevoflurane-induced long-term cognitive disorders [38, 39]. Besides, the function of N-Methyl-d-aspartate (NMDA) receptors which is critical for learning and memory has been interfered by repeated sevoflurane anesthesia at the neonatal stage [40, 41]. On the other hand, sevoflurane-

induced neurotoxicity was alleviated by treatments of tanshinone IIA, dexmedetomidine, or JNK inhibitor [42–44]. In this study, MWM and social interaction tests confirmed that multiple exposures to sevoflurane in the neonatal period induced cognitive impairment in the young mice. Moreover, RNA-seq analysis of the hippocampus revealed several genes and biological processes related to brain development, including

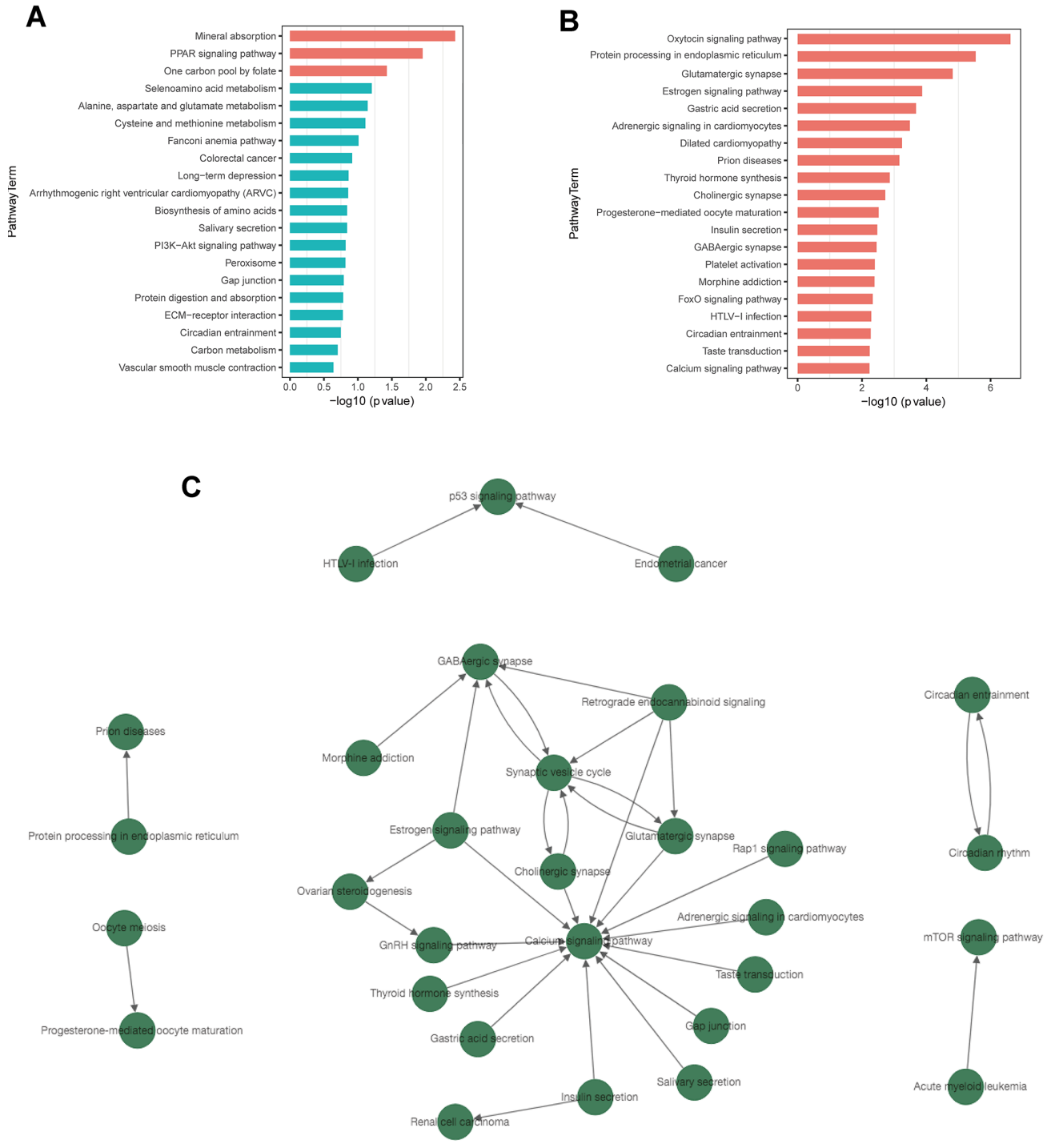

Figure 5. KEGG pathway enrichment and pathway-tree analysis. (**A**) Top 20 enriched pathways of up-regulated DEGs. (**B**) Top 20 enriched pathways of down-regulated DEGs. (**C**) Pathway-tree analysis showing relationship between pathway terms. Arrow source, an upstream signal pathway; arrow target, a downstream signaling pathway. Blue columns indicate pathways without significant difference.

nervous system development (GO:0007399; *Igsf9, Ina, Pou3f3, Sema7a, Nes, Nr2f1, Lmtk2, Fezf2, Cit, Ndel1, Brsk1, Nrsn1, Gdpd5, Sema6c, Bax, Pten*), exocytosis (GO:0006887; *Stxbp1, Doc2a, Cdk16, Stx1a, Rims3, Srcin1, Rims4, Cplx1*), synapse assembly (GO:0007416; *Plxnd1, Farp1, Shank2, Clstn3, Pten*), and phosphorylation (GO:0016310; *Camk2n2, Prkar1b, Fgfr3, Ulk1, Limk1, Adrbk1, Cdk16, Pink1, Lmtk2, Stk32c, Nlk, Cit, Brsk1, Pik3cd, Ttbk1, Pak6, Camkk2, Tnk2, Mast2, Csnk1e, Sbk1, Cerk*). In addition, there were several biological processes related to learning and memory, including learning (GO:0007612; *Grm4*, *Ctnnd2*, *Pak6*, *Shank2*), memory (GO:0007613; *Adrb1*, *Pak6*, *Shank2*, *Pten*), learning or memory (GO:0007611; *Prkar1b*, *Egr1*, *Pten*), and long-term memory (GO:0007616; *Adcy1*, *Adcy8*). Of note, all the above-mentioned genes were significantly down-regulated in the hippocampus of sevoflurane-treated mice, suggesting potential new mechanisms which underlie the cognitive impairment by sevoflurane exposure.

In the GO analysis, several top enriched biological processes were related to ion channels. Cellular zinc ion homeostasis (GO:0006882; *Adamts3, Ccbe1*), zinc ion transport (GO:0006829; *Slc30a1, Slc30a10*), and negative regulation of zinc ion transmembrane import (GO:0071584; *Slc30a1*) were associated with up-regulated DEGs. Regulation of ion transmembrane transport (GO:0034765; *Cacng2, Kcnh3, Kcna3, Kcnj4, Cacna1i, Kcnc4, Kcnab3, Kcnj11, Scn1b, Kcnj9, Kcnf1, Kcnb1, Cacng7, Kcnk3, Kcnc1, Kcnj2*), potassium ion transmembrane transport (GO:0071805; *Kcnh3, Kcna3, Kcnk12, Kcnj4, Kcnc4, Kcnab3, Kcnj11, Kcnf1, Kcnb1, Kcnk3, Kcnc1, Kcnj2*), potassium ion transport (GO:0006813; *Kcnh3, Kcna3, Kcnj4, Kcnc4, Kcnab3, Kcnj11, Kcnj9, Kcnf1, Kcnb1, Kcnk3, Kcnc1, Kcnj2*), and ion transport (GO:0006811; *Cacng2, Kcnh3, Kcna3, Slc38a2, Kcnk12, Kcnj4, Cacna1i, Lasp1, Kcnc4, Fxyd7, Kcnab3, Kcnj11, Grid1, Scn1b, Kcnj9, Kcnf1, Kcnb1, Cacng7, Kcnk3, Kcnc1, Kcnj2*) were based on down-regulated DEGs. Consistently, previous findings support that sevoflurane could influence the activities of ion channels [45–48].

Cellular response to hypoxia and apoptotic process are also involved in the effects of sevoflurane on the neonatal brain. We found enriched biological process of cellular response to hypoxia associated with down-regulated DEGs (GO:0071456; *Egr1, Pink1, Ppard, Kcnk3*). Previous studies showed that early exposure to

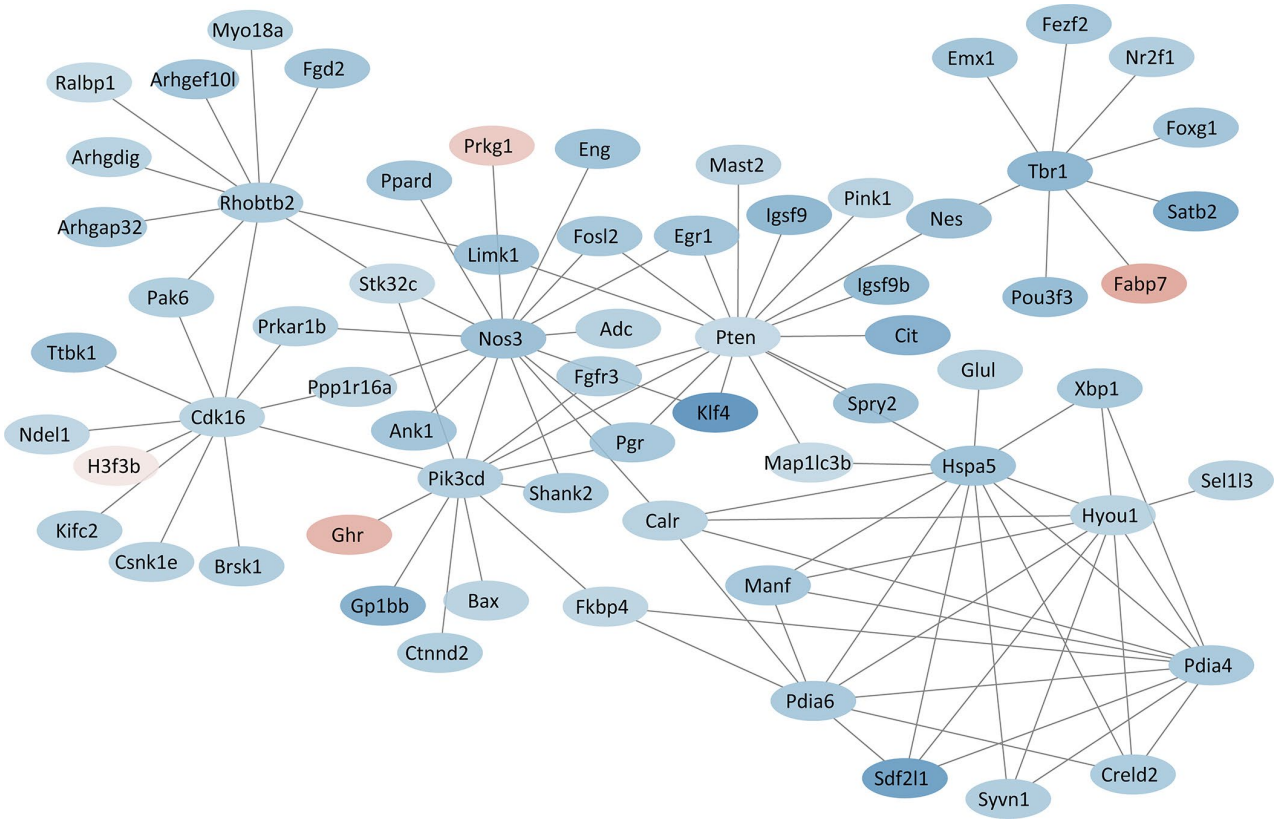

Figure 6. PPI network based on hub proteins. Red and blue colors indicate proteins with up- and down-regulated expression, respectively.

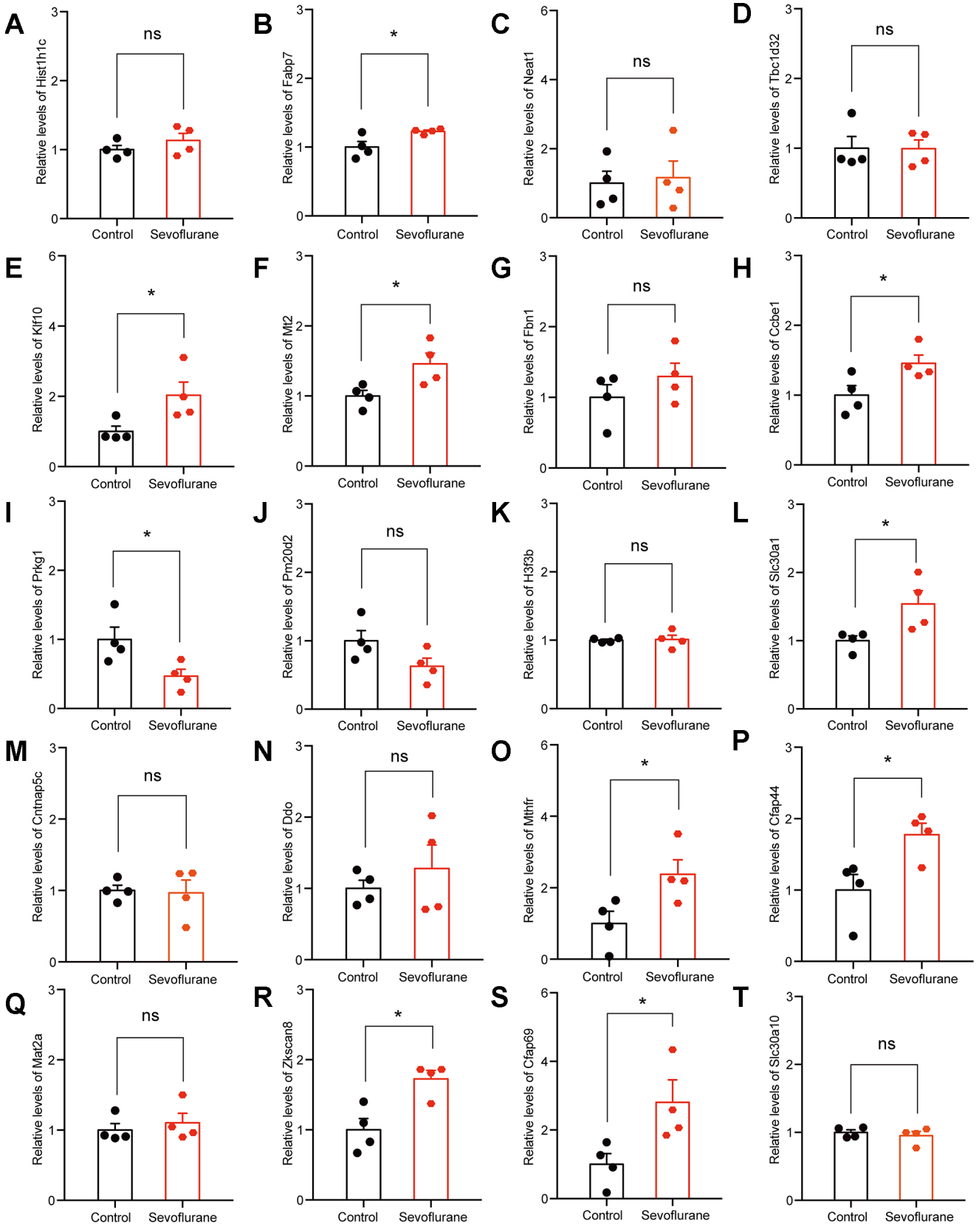

Figure 7. qPCR verification of top 20 up-regulated DEGs. (**A**) *Hist1h1c*. (**B**) *Fabp7*. (**C**) *Neat1*. (**D**) *Tbc1d32*. (**E**) *Klf10*. (**F**) *Mt2*. (**G**) *Fbn1*. (**H**) *Ccbe1*. (**I**) *Prkg1*. (**J**) *Pm20d2*. (**K**) *H3f3b*. (**L**) *Slc30a1*. (**M**) *Cntnap5c*. (**N**) *Ddo*. (**O**) *Mthfr*. (**P**) *Cfap44*. (**Q**) *Mat2a*. (**R**) *Zkscan8*. (**S**) *Cfap69*. (**T**) *Slc30a10*. n = 4. *$p < 0.05$ for the comparisons shown.

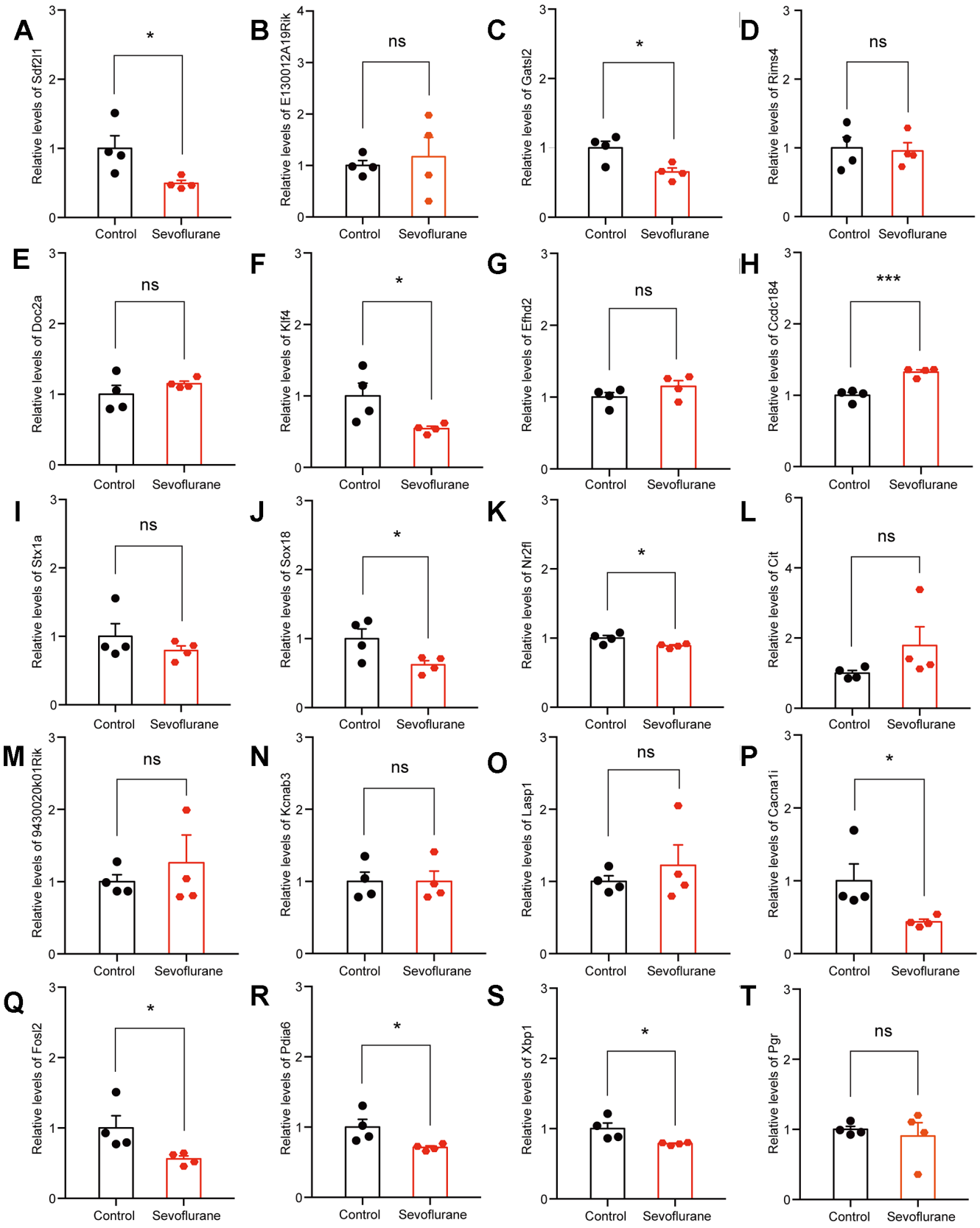

Figure 8. qPCR verification of top 20 down-regulated DEGs. (**A**) *Sdf2l1*. (**B**) *E130012A19Rik*. (**C**) *Gatsl2*. (**D**) *Rims4*. (**E**) *Doc2a*. (**F**) *Klf4*. (**G**) *Efhd2*. (**H**) *Ccdc184*. (**I**) *Stx1a*. (**J**) *Sox18*. (**K**) *Nr2f1*. (**L**) *Cit*. (**M**) *9430020K01Rik*. (**N**) *Kcnab3*. (**O**) *Lasp1*. (**P**) *Cacna1i*. (**Q**) *Fosl2*. (**R**) *Pdia6*. (**S**) *Xbp1*. (**T**) *Pgr*. n = 4. *$p < 0.05$, ***$p < 0.001$ for the comparisons shown.

sevoflurane could cause apoptosis in the cerebral cortex and hippocampus [49, 50]. In this study, the GO analysis revealed a number of biological processes related to apoptosis, such as regulation of neuron apoptotic process (GO:0043523; *Grm2, Pink1, Bax*), positive regulation of apoptotic process (GO:0043065; *Adrb1, Zbtb16, Bcl6, Dab2ip, Zmat3, Nos3, Bax, Pten*), positive regulation of neuron apoptotic process (GO:0043525; *Fgfr3, Egr1, Bax*), and negative regulation of neuron apoptotic process (GO:0043524; *Stxbp1, Nes, Pink1, Bax, Sncb*). These results suggest that multiple sevoflurane exposures may affect neurodevelopment through regulating cellular response to hypoxia and the apoptotic process.

Autism spectrum disorder (ASD), a common childhood neurodevelopmental disorder, is characterized by social interaction impairment and repetitive behaviors [51]. It is unclear whether sevoflurane exposure may contribute to the development of ASD. Some studies reported that neonatal exposures to sevoflurane induced abnormal social behaviors [31, 52, 53], while others found no autism-like behaviors after sevoflurane anesthesia [36, 54]. In this study, multiple neonatal exposures to sevoflurane had a negative impact on social interactions, evidence by the loss of ability to distinguish a new mouse. This result can also be explained by the impairments of the frontal cortex functions, which is most vulnerable in the observed period of ontogenesis. A recent study found that multiple sevoflurane anesthesia impaired the prefrontal cortex functions in the developmental brain [55]. Our RNA-seq analysis identified 3 down-regulated genes (*Grid1*, *Shank2*, *Pten*) related to social behaviors, 5 down-regulated genes (*Sobp*, *Fezf2*, *Pak6*, *Apba1*, *Pten*) related to locomotory behaviors, and 1 up-regulated gene (*Ddo*) related to grooming-like stereotyped behaviors. The current results may help to detect the key genes for ASD treatment in further investigations.

Among the significantly enriched signaling pathways from KEGG analysis, oxytocin signaling pathway (PATH:04921; *Cacng2, Adcy1, Kcnj4, Kcnj9, Adcy8, Pik3cd, Elk1, Adcy4, Camkk2, Cacng7, Nos3, Kcnj2*) may play an important role in the sevoflurane-induced cognitive impairment. Tara et al. found that oxytocin signaling pathway in the hippocampus was essential for social recognition [56]. In this study, a significantly decreased activity of oxytocin signaling in the hippocampus was noted. In addition, several enriched signaling pathways of down-regulated DEGs were on the regulation of synapses, including glutamatergic synapse (PATH:04724; *Slc38a2, Grm4, Adcy1, Grm2, Adrbk1, Glul, Adcy8, Adcy4, Shank2*), cholinergic synapse (PATH:04725; *Adcy1, Kcnj4, Adcy8, Pik3cd, Adcy4, Kcnj2*), and GABAergic synapse (PATH:04727; *Slc38a2, Adcy1, Glul, Adcy8, Adcy4*). The above-mentioned pathways and related genes may be useful for further research.

The PPI network revealed several hub-proteins encoded by DEGs, including phosphatase and tensin homolog (Pten), nitric oxide synthase 3 (Nos3), phosphatidylinositol-4,5-bisphosphate 3-kinase catalytic subunit delta (Pik3cd), cyclin-dependent kinase 16 (Cdk16), Rho-related BTB domain containing 2 (Rhobtb2), hypoxia up-regulated 1 (Hyou1), heat shock protein 5 (Hspa5), protein disulfide isomerase associated 4 (Pdia4), protein disulfide isomerase associated 6 (Pdia6), and T-box brain gene 1 (Tbr1). Among these, Pten was involved in the processes of nervous system development, synapse assembly, learning and memory, and locomotory and social behaviors in the GO analysis. A recent study found that sevoflurane exposure on gestational day 14 induced neurotoxicity in the fetal brain of rats through the Pten signaling [57]. For other hub-proteins, Nos3 and Pik3cd were involved in the oxytocin signaling pathway in the KEGG analysis, and Cdk16 was involved in exocytosis and phosphorylation. Recent studies also showed that Nos3 and Pik3cd play an important role in neurodevelopmental disorders [58, 59].

This study has several limitations. First, the RNA-seq only tested the expression profile of mRNAs, without other types of RNAs such as lncRNAs or miRNAs. Second, the sample size of RNA-seq analysis was relatively small. Third, there were variations in gene expression detected by RNA-seq and qPCR, which may be due to the methodological or statistical differences. Fourth, the transcriptomic profile may need to be further validated by using the western blot experiment. Last, the entire hippocampal tissues of mice were harvested for RNA-seq. The discrepancy of gene expression and signaling pathway enrichment among different hippocampal regions including cornu amonis (CA)1, CA2, CA3, and gyrus dentatus should be considered. Therefore, based on the current findings, further experiments with larger sample size are needed to identify the role of key genes in response to multiple neonatal sevoflurane exposures.

In summary, multiple neonatal exposures to sevoflurane induced cognitive impairment and social behavior disorders in young mice. RNA-seq analysis identified 314 DEGs that encode proteins participating in relevant biological processes (ion channels, brain development, synapse assembly, learning, and memory) and signaling pathways (oxytocin signaling pathway, glutamatergic synapse, cholinergic synapse, and GABAergic synapse), via which the mice hippocampus responded to sevoflurane. With a novel insight into the sevoflurane-related neurotoxicity in developing brain, this study helps to provide a fundamental work for elucidation of

underlying mechanisms and exploration of potential prophylactic targets.

MATERIALS AND METHODS

Animals and sevoflurane anesthesia

The experimental protocol was approved (protocol number: 201808A076) by the Institutional Animal Care and Use Committee of Soochow University (Suzhou, China). C57BL/6J mice were purchased from the Slaccas Laboratory (Shanghai, China) and received standard rodent food and water. The male pups were used in this study. Using a computer-generated table, the neonatal mice were randomly assigned to either of the two study groups (control or sevoflurane).

The animal model was described in a recent study [12]. On PND 6, 8, and 10, the sevoflurane group received 3% sevoflurane with 60% oxygen (balanced with nitrogen) for 2 h (2 L/min fresh gas for 3 min, followed by 1 L/min) in a chamber using the Datex-Ohmeda anesthesia system (Madison, WI, USA), while the control group received 60% oxygen in nitrogen for 2 h. The sevoflurane concentration was monitored and adjusted by using a gas analyzer (Vamos; Dräger Medical, Germany). The rectal temperature of mice was maintained at 37 ± 0.5 °C. After treatment, the mice were returned to home cages under standard care.

Arterial blood gas analysis

Blood samples (100 μL each) were taken from the abdominal aorta at 5 min and 115 min during sevoflurane exposure on PND 10 (n = 8 for each group). The samples were then immediately analyzed by using a blood gas analyzer (Radiometer, ABL80 FLEX, Carlsbad, CA, USA). The values of pH, partial pressures of oxygen (PO_2) and carbon dioxide (PCO_2), hematocrit (Hct), Na^+, K^+, Ca^{2+}, and Cl^- were recorded.

Behavioral studies

The behavioral tests (n = 10 for each group) in this study included MWM at 03:00-5:00 pm on PND 31–36, social interaction test at 09:00-12:00 am on PND 31, open field test at 09:00-11:00 am on PND 32, elevated plus maze at 09:00-11:00 am on PND 33, light-dark box test at 09:00-11:00 am on PND 34, and self-grooming test at 09:00-11:00 am on PND 35. The motions of each mouse were monitored and recorded by the ANY-maze Behavior Tracking System (Stoelting Co., Wood Dale, IL, USA).

MWM tests were conducted as previously described [60]. The water maze device was filled with opaque water using titanium dioxide to reach the level of 1.0 cm above the surface of a platform (diameter, 10 cm). Throughout the experiment, the water temperature was kept at 22 °C, and the surrounding environment remained quiet. In the training phase on PND 31–35, the mice were trained to reach the platform for 5 days with 4 trials per day, and the escape latency (time for mice to reach the platform) was recorded for the evaluation of spatial learning. In the testing phase on PND 36, the platform was removed, and mean distance from the original platform area, platform-crossing times, and time spent in the fourth quadrant (the platform quadrant) were recorded for the assessment of memory function. A heat lamp was used to warm and dry the mice before returning to home cages.

Social interaction tests were performed as previously presented [61]. In the first session (habituation), the mouse was initially placed in the middle chamber, with free access to the left and right chambers. During 5 min of observation, the time of sniffing (direct snout-to-enclosure contact) at both enclosures in the center of chambers was recorded. In the second session (sociability), a different mouse, Stranger 1, was placed into one enclosure, and the motions of the experiment mouse were tracked for 10 min. The time of sniffing at Stranger 1 and at the empty enclosure were recorded. In the third session (preference for social novelty), another mouse, Stranger 2, was placed into the other enclosure, and the motions of the experiment mouse was tracked for 10 min. The time of sniffing at Stranger 1 and Stranger 2 was recorded.

Open field tests were carried out to investigate the anxiety-like and exploratory behaviors, according to the previously described methods [62]. A central area of 10 × 10 cm^2 was defined in the field box (40 × 40 × 40 cm^3). The mouse was initially placed in the corner of the box and allowed to explore the field freely for 10 min. The time spent in the central area, speed of movement, and distance travelled were recorded.

Elevated plus maze and light-dark box tests were used to assess the depression-like behaviors [63, 64]. The mouse was initially placed at the center of the maze and allowed to explore the maze freely for 10 min. The time of exploring open arms and number of open and closed arms entries were recorded. For the light-dark box, a large bright compartment was connected to a small caliginous compartment by a door of 7 cm. The mouse was initially placed in the center of the bright compartment and allowed to explore the two compartments freely for 5 min. The time spent in the caliginous compartment was recorded.

Self-grooming tests were performed to evaluate the stereotyped behaviors using the previously described

methods [65]. The mouse was housed individually and habituated to the circumstances in the open field box. Self-grooming behaviors (elliptical strokes, small strokes, bilateral strokes, flank licks, and tail and genital licks) [66], were tracked for 10 min. The numbers and time of self-grooming of each mouse were recorded.

RNA isolation and sequencing

Total RNA was isolated from the mouse hippocampus using the Trizol reagent (Ambion, Shanghai, China). RNA purity and concentration were evaluated by using the Nanodrop ND-2000 spectrophotometer (Thermo Fisher Scientific, Waltham, MA, USA). RNA purity and integrity were checked by 1.5% agarose gel electrophoresis. RNA Integrity Number value > 7.0 was confirmed by using the Agilent 2100 Bioanalyzer (Agilent Technologies, Santa Clara, CA, USA).

Sequencing library was generated by using the TruSeq RNA preparation kit (Illumina, San Diego, CA, USA), following the manufacturer's protocols. In Brief, the mRNA was purified by Oligo (dT) magnetic beads and fragmented into 200 bp short fragments. The complementary DNA (cDNA) was synthesized and purified. The concentration of cDNA was assessed by using the Qubit 2.0 (Thermo Fisher Scientific, Waltham, MA, USA), and the length of library fragments was determined by using the Agilent 2100 Bioanalyzer. Finally, sequencing was performed by using an Illumina HiSeq 2500 platform (Illumina, San Diego, CA, USA) and 125 bp paired-end reads were generated.

Quality assessment of raw RNA-seq data

The raw data derived from RNA-seq was analyzed by using the FastQC (version 0.11.8, Babraham Bioinformatics, Babraham Institute, Cambridge, UK). To obtain the high-quality clean reads for subsequent analysis, the low-quality reads including the adaptor sequences, sequences with quality score of < 20, and reads with > 5% ambiguous bases (N bases) were removed from the sequencing data by using the Cutadapt v2.3 [67]. The raw data was uploaded onto the National Center for Biotechnology Information (NCBI), with the accession number of PRJNA556843 (available at: https://dataview.ncbi.nlm.nih.gov/object/PRJNA556843) .

Identification of DEGs

The clean reads from RNA-seq were aligned to mm10_UCSC genome by using the STAR tool [68]. Reads Per Kb per Million reads (RPKM) was used for the normalization and calculation of gene expression, and the DESeq2 algorithm (http://bioconductor.org/packages/DESeq2/) was applied to filter the DEGs [69]. The raw *p*-value was adjusted to false discovery rate (FDR), and FDR < 0.05 was considered as the cut-off criteria for DEGs screening [70]. To get an inclusive set of DEGs, we did not apply a fold change threshold for DEGs screening [71–74]. To overview the characteristics of gene expression profiles, volcano plots and heatmaps were generated by using the R package.

Functional annotation of DEGs

GO analysis was performed to evaluate the functional enrichment of DEGs in the biological process, cellular component, and molecular function [75]. The annotations were downloaded from NCBI (www.ncbi.nlm.nih.gov/), UniProt (www.uniprot.org/), and Gene Ontology (www.geneontology.org/). A *p*-value < 0.05 was set as the threshold value. In addition, GO-Tree was constructed based on the significant GO-terms of DEGs. The GO-Tree is a directed acyclic graph, showing the relationships of GO-terms [76].

Kyoto Encyclopedia of Genes and Genomes (KEGG) pathway analysis was performed to analyze the enriched signaling pathways of DEGs based on the KEGG database (www.genome.jp/kegg/) [77]. A *p*-value < 0.05 was set as the threshold value. In addition to gene annotation in signaling pathways, the upstream and downstream relationships of the enriched pathways were shown by pathway network analysis.

Protein-protein interaction network integration

The interactions among the proteins translated from the DEGs were analyzed by using the STRING database (version 10.5; www.string-db.org/), and the PPI network was visualized by using the Cytoscape software (www.cytoscape.org/) [78]. The proteins in the central node (hub proteins) may be the key proteins or genes that play an important role in regulating the physiological functions.

qPCR

RNA was extracted from the mouse hippocampus (n = 4 for each group), and cDNA was synthesized using a reverse transcription kit (Transgen Biotech, Beijing, China). qPCR was carried out with the SYBR Green MasterMix in a 20 μL reaction volume by using the 7500 Fast Real-Time PCR System (Applied Biosystems, Bedford, MA, USA). Primers specific to the top 20 up- and down-regulated DEGs were synthesized by the Sangon Biotech (Shanghai, China), as shown in Supplementary Table 1. GAPDH was used as an internal control. Cycle threshold (Ct) value of a gene was obtained, and gene abundance was determined by using the $2^{-\Delta\Delta Ct}$ method.

Statistical analysis

Data obtained from blood gas analysis, behavioral studies, and qPCR were checked for normal distribution and presented as mean ± standard error of the mean (SEM). Data were analyzed using the unpaired student's *t* test or two-way analysis of variance (ANOVA) with repeated measurement followed by Bonferroni's post hoc test as appropriate. All analyses were performed by using the GraphPad Prism 7.0 (San Diego, CA, USA). A two-tailed *p*-value < 0.05 indicates a statistically significant difference.

CONFLICTS OF INTEREST

The authors have no conflicts of interest.

FUNDING

This study was supported by National Natural Science Foundation of China (81601659 to KP, 81873925 and 81671880 to FHJ, 81601666 to JZ, and 81701098 to XWM), Jiangsu Provincial Medical Youth Talents Program (QNRC2016741 to KP), Jiangsu Provincial Medical Innovation Team (CXTDA2017043 to FHJ), and Suzhou Key Disease Program (LCZX201603 to FHJ).

REFERENCES

1. Shi Y, Hu D, Rodgers EL, Katusic SK, Gleich SJ, Hanson AC, Schroeder DR, Flick RP, Warner DO. Epidemiology of general anesthesia prior to age 3 in a population-based birth cohort. Paediatr Anaesth. 2018; 28:513–19. https://doi.org/10.1111/pan.13359 PMID:29532559

2. Vinson AE, Houck CS. Neurotoxicity of Anesthesia in Children: prevention and Treatment. Curr Treat Options Neurol. 2018; 20:51. https://doi.org/10.1007/s11940-018-0536-z PMID:30315440

3. Kain ZN, Mayes LC, Caldwell-Andrews AA, Karas DE, McClain BC. Preoperative anxiety, postoperative pain, and behavioral recovery in young children undergoing surgery. Pediatrics. 2006; 118:651–58. https://doi.org/10.1542/peds.2005-2920 PMID:16882820

4. Wilder RT, Flick RP, Sprung J, Katusic SK, Barbaresi WJ, Mickelson C, Gleich SJ, Schroeder DR, Weaver AL, Warner DO. Early exposure to anesthesia and learning disabilities in a population-based birth cohort. Anesthesiology. 2009; 110:796–804. https://doi.org/10.1097/01.anes.0000344728.34332.5d PMID:19293700

5. Sun L. Early childhood general anaesthesia exposure and neurocognitive development. Br J Anaesth. 2010 (Suppl 1); 105:i61–68. https://doi.org/10.1093/bja/aeq302 PMID:21148656

6. Vutskits L, Xie Z. Lasting impact of general anaesthesia on the brain: mechanisms and relevance. Nat Rev Neurosci. 2016; 17:705–17. https://doi.org/10.1038/nrn.2016.128 PMID:27752068

7. Glatz P, Sandin RH, Pedersen NL, Bonamy AK, Eriksson LI, Granath F. Association of Anesthesia and Surgery During Childhood With Long-term Academic Performance. JAMA Pediatr. 2017; 171:e163470. https://doi.org/10.1001/jamapediatrics.2016.3470 PMID:27820621

8. Davidson AJ, Disma N, de Graaff JC, Withington DE, Dorris L, Bell G, Stargatt R, Bellinger DC, Schuster T, Arnup SJ, Hardy P, Hunt RW, Takagi MJ, et al, and GAS consortium. Neurodevelopmental outcome at 2 years of age after general anaesthesia and awake-regional anaesthesia in infancy (GAS): an international multicentre, randomised controlled trial. Lancet. 2016; 387:239–50. https://doi.org/10.1016/S0140-6736(15)00608-X PMID:26507180

9. Sun LS, Li G, Miller TL, Salorio C, Byrne MW, Bellinger DC, Ing C, Park R, Radcliffe J, Hays SR, DiMaggio CJ, Cooper TJ, Rauh V, et al. Association Between a Single General Anesthesia Exposure Before Age 36 Months and Neurocognitive Outcomes in Later Childhood. JAMA. 2016; 315:2312–20. https://doi.org/10.1001/jama.2016.6967 PMID:27272582

10. McCann ME, de Graaff JC, Dorris L, Disma N, Withington D, Bell G, Grobler A, Stargatt R, Hunt RW, Sheppard SJ, Marmor J, Giribaldi G, Bellinger DC, et al, and GAS Consortium. Neurodevelopmental outcome at 5 years of age after general anaesthesia or awake-regional anaesthesia in infancy (GAS): an international, multicentre, randomised, controlled equivalence trial. Lancet. 2019; 393:664–77. https://doi.org/10.1016/S0140-6736(18)32485-1 PMID:30782342

11. Warner DO, Zaccariello MJ, Katusic SK, Schroeder DR, Hanson AC, Schulte PJ, Buenvenida SL, Gleich SJ, Wilder RT, Sprung J, Hu D, Voigt RG, Paule MG, et al. Neuropsychological and Behavioral Outcomes after Exposure of Young Children to Procedures Requiring General Anesthesia: The Mayo Anesthesia Safety in Kids (MASK) Study. Anesthesiology. 2018; 129:89–105. https://doi.org/10.1097/ALN.0000000000002232 PMID:29672337

12. Lu H, Liufu N, Dong Y, Xu G, Zhang Y, Shu L, Soriano SG, Zheng H, Yu B, Xie Z. Sevoflurane Acts on Ubiquitination-Proteasome Pathway to Reduce

Postsynaptic Density 95 Protein Levels in Young Mice. Anesthesiology. 2017; 127:961–75. https://doi.org/10.1097/ALN.0000000000001889 PMID:28968276

13. Lei X, Guo Q, Zhang J. Mechanistic insights into neurotoxicity induced by anesthetics in the developing brain. Int J Mol Sci. 2012; 13:6772–99. https://doi.org/10.3390/ijms13066772 PMID:22837663

14. Jevtovic-Todorovic V, Hartman RE, Izumi Y, Benshoff ND, Dikranian K, Zorumski CF, Olney JW, Wozniak DF. Early exposure to common anesthetic agents causes widespread neurodegeneration in the developing rat brain and persistent learning deficits. J Neurosci. 2003; 23:876–82. https://doi.org/10.1523/JNEUROSCI.23-03-00876.2003 PMID:12574416

15. Hofacer RD, Deng M, Ward CG, Joseph B, Hughes EA, Jiang C, Danzer SC, Loepke AW. Cell age-specific vulnerability of neurons to anesthetic toxicity. Ann Neurol. 2013; 73:695–704. https://doi.org/10.1002/ana.23892 PMID:23526697

16. Yu D, Liu B. Developmental anesthetic neurotoxicity: from animals to humans? J Anesth. 2013; 27:750–56. https://doi.org/10.1007/s00540-013-1609-5 PMID:23588921

17. Wang X, Dong Y, Zhang Y, Li T, Xie Z. Sevoflurane induces cognitive impairment in young mice via autophagy. PLoS One. 2019; 14:e0216372. https://doi.org/10.1371/journal.pone.0216372 PMID:31107909

18. Gibert S, Sabourdin N, Louvet N, Moutard ML, Piat V, Guye ML, Rigouzzo A, Constant I. Epileptogenic effect of sevoflurane: determination of the minimal alveolar concentration of sevoflurane associated with major epileptoid signs in children. Anesthesiology. 2012; 117:1253–61. https://doi.org/10.1097/ALN.0b013e318273e272 PMID:23103557

19. Ji MH, Wang ZY, Sun XR, Tang H, Zhang H, Jia M, Qiu LL, Zhang GF, Peng YG, Yang JJ. Repeated Neonatal Sevoflurane Exposure-Induced Developmental Delays of Parvalbumin Interneurons and Cognitive Impairments Are Reversed by Environmental Enrichment. Mol Neurobiol. 2017; 54:3759–70. https://doi.org/10.1007/s12035-016-9943-x PMID:27251428

20. Xu G, Lu H, Dong Y, Shapoval D, Soriano SG, Liu X, Zhang Y, Xie Z. Coenzyme Q10 reduces sevoflurane-induced cognitive deficiency in young mice. Br J Anaesth. 2017; 119:481–91. https://doi.org/10.1093/bja/aex071 PMID:28482003

21. Liu G, Zhu T, Zhang A, Li F, Qian W, Qian B. Heightened stress response and cognitive impairment after repeated neonatal sevoflurane exposures might be linked to excessive GABAAR-mediated depolarization. J Anesth. 2016; 30:834–41. https://doi.org/10.1007/s00540-016-2215-0 PMID:27435414

22. Neves G, Cooke SF, Bliss TV. Synaptic plasticity, memory and the hippocampus: a neural network approach to causality. Nat Rev Neurosci. 2008; 9:65–75. https://doi.org/10.1038/nrn2303 PMID:18094707

23. Epstein RA, Patai EZ, Julian JB, Spiers HJ. The cognitive map in humans: spatial navigation and beyond. Nat Neurosci. 2017; 20:1504–13. https://doi.org/10.1038/nn.4656 PMID:29073650

24. Pastalkova E, Serrano P, Pinkhasova D, Wallace E, Fenton AA, Sacktor TC. Storage of spatial information by the maintenance mechanism of LTP. Science. 2006; 313:1141–44. https://doi.org/10.1126/science.1128657 PMID:16931766

25. Tsien JZ, Huerta PT, Tonegawa S. The essential role of hippocampal CA1 NMDA receptor-dependent synaptic plasticity in spatial memory. Cell. 1996; 87:1327–38. https://doi.org/10.1016/S0092-8674(00)81827-9 PMID:8980238

26. Morrison JH, Baxter MG. The ageing cortical synapse: hallmarks and implications for cognitive decline. Nat Rev Neurosci. 2012; 13:240–50. https://doi.org/10.1038/nrn3200 PMID:22395804

27. Kolosova NG, Vitovtov AO, Muraleva NA, Akulov AE, Stefanova NA, Blagosklonny MV. Rapamycin suppresses brain aging in senescence-accelerated OXYS rats. Aging (Albany NY). 2013; 5:474–84. https://doi.org/10.18632/aging.100573 PMID:23817674

28. Ing C, DiMaggio C, Whitehouse A, Hegarty MK, Brady J, von Ungern-Sternberg BS, Davidson A, Wood AJ, Li G, Sun LS. Long-term differences in language and cognitive function after childhood exposure to anesthesia. Pediatrics. 2012; 130:e476–85. https://doi.org/10.1542/peds.2011-3822 PMID:22908104

29. Li Y, Liu C, Zhao Y, Hu K, Zhang J, Zeng M, Luo T, Jiang W, Wang H. Sevoflurane induces short-term changes in proteins in the cerebral cortices of developing rats. Acta Anaesthesiol Scand. 2013; 57:380–90. https://doi.org/10.1111/aas.12018 PMID:23186353

30. Zhou X, Song FH, He W, Yang XY, Zhou ZB, Feng X, Zhou LH. Neonatal exposure to sevoflurane causes apoptosis

and reduces nNOS protein expression in rat hippocampus. Mol Med Rep. 2012; 6:543–46. https://doi.org/10.3892/mmr.2012.976 PMID:22751864

31. Satomoto M, Satoh Y, Terui K, Miyao H, Takishima K, Ito M, Imaki J. Neonatal exposure to sevoflurane induces abnormal social behaviors and deficits in fear conditioning in mice. Anesthesiology. 2009; 110:628–37. https://doi.org/10.1097/ALN.0b013e3181974fa2 PMID:19212262

32. Lu Y, Wu X, Dong Y, Xu Z, Zhang Y, Xie Z. Anesthetic sevoflurane causes neurotoxicity differently in neonatal naïve and Alzheimer disease transgenic mice. Anesthesiology. 2010; 112:1404–16. https://doi.org/10.1097/ALN.0b013e3181d94de1 PMID:20460993

33. D'Hooge R, De Deyn PP. Applications of the Morris water maze in the study of learning and memory. Brain Res Brain Res Rev. 2001; 36:60–90. https://doi.org/10.1016/S0165-0173(01)00067-4 PMID:11516773

34. Yu Y, Zhang P, Yan J, Sun Y, Wu X, Xi S, Zhang L, Sun Y, Hu R, Jiang H. Sevoflurane induces cognitive impairments via the MiR-27b/LIMK1-signaling pathway in developing rats. Inhal Toxicol. 2016; 28:731–38. https://doi.org/10.1080/08958378.2016.1266532 PMID:27973945

35. Satomoto M, Sun Z, Adachi YU, Makita K. Neonatal Sevoflurane Exposure Induces Adulthood Fear-induced Learning Disability and Decreases Glutamatergic Neurons in the Basolateral Amygdala. J Neurosurg Anesthesiol. 2018; 30:59–64. https://doi.org/10.1097/ana.0000000000000387 PMID:27820300

36. Chung W, Park S, Hong J, Park S, Lee S, Heo J, Kim D, Ko Y. Sevoflurane exposure during the neonatal period induces long-term memory impairment but not autism-like behaviors. Paediatr Anaesth. 2015; 25:1033–45. https://doi.org/10.1111/pan.12694 PMID:26095314

37. Zhao X, Jin Y, Li H, Jia Y, Wang Y. Sevoflurane impairs learning and memory of the developing brain through post-transcriptional inhibition of CCNA2 via microRNA-19-3p. Aging (Albany NY). 2018; 10:3794–805. https://doi.org/10.18632/aging.101673 PMID:30540563

38. Ando N, Sugasawa Y, Inoue R, Aosaki T, Miura M, Nishimura K. Effects of the volatile anesthetic sevoflurane on tonic GABA currents in the mouse striatum during postnatal development. Eur J Neurosci. 2014; 40:3147–57. https://doi.org/10.1111/ejn.12691 PMID:25139222

39. Li T, Huang Z, Wang X, Zou J, Tan S. Role of the GABAA receptors in the long-term cognitive impairments caused by neonatal sevoflurane exposure. Rev Neurosci. 2019. [Epub ahead of print]. https://doi.org/10.1515/revneuro-2019-0003 PMID:31145696

40. Wang WY, Jia LJ, Luo Y, Zhang HH, Cai F, Mao H, Xu WC, Fang JB, Peng ZY, Ma ZW, Chen YH, Zhang J, Wei Z, et al. Location- and Subunit-Specific NMDA Receptors Determine the Developmental Sevoflurane Neurotoxicity Through ERK1/2 Signaling. Mol Neurobiol. 2016; 53:216–30. https://doi.org/10.1007/s12035-014-9005-1 PMID:25421211

41. Zhang X, Shen F, Xu D, Zhao X. A lasting effect of postnatal sevoflurane anesthesia on the composition of NMDA receptor subunits in rat prefrontal cortex. Int J Dev Neurosci. 2016; 54:62–69. https://doi.org/10.1016/j.ijdevneu.2016.01.008 PMID:27025552

42. Xia Y, Xu H, Jia C, Hu X, Kang Y, Yang X, Xue Q, Tao G, Yu B. Tanshinone IIA Attenuates Sevoflurane Neurotoxicity in Neonatal Mice. Anesth Analg. 2017; 124:1244–52. https://doi.org/10.1213/ANE.0000000000001942 PMID:28319548

43. Perez-Zoghbi JF, Zhu W, Grafe MR, Brambrink AM. Dexmedetomidine-mediated neuroprotection against sevoflurane-induced neurotoxicity extends to several brain regions in neonatal rats. Br J Anaesth. 2017; 119:506–16. https://doi.org/10.1093/bja/aex222 PMID:28969317

44. Bi C, Cai Q, Shan Y, Yang F, Sun S, Wu X, Liu H. Sevoflurane induces neurotoxicity in the developing rat hippocampus by upregulating connexin 43 via the JNK/c-Jun/AP-1 pathway. Biomed Pharmacother. 2018; 108:1469–1476. https://doi.org/10.1016/j.biopha.2018.09.111 PMID:30372849

45. Stock L, Hosoume J, Cirqueira L, Treptow W. Binding of the general anesthetic sevoflurane to ion channels. PLOS Comput Biol. 2018; 14:e1006605. https://doi.org/10.1371/journal.pcbi.1006605 PMID:30475796

46. Woll KA, Peng W, Liang Q, Zhi L, Jacobs JA, Maciunas L, Bhanu N, Garcia BA, Covarrubias M, Loll PJ, Dailey WP, Eckenhoff RG. Photoaffinity Ligand for the Inhalational Anesthetic Sevoflurane Allows Mechanistic Insight into Potassium Channel Modulation. ACS Chem Biol. 2017; 12:1353–62. https://doi.org/10.1021/acschembio.7b00222

PMID:28333442

47. Liu Y, Yang H, Tang X, Bai W, Wang G, Tian X. Repetitive transcranial magnetic stimulation regulates L-type Ca(2+) channel activity inhibited by early sevoflurane exposure. Brain Res. 2016; 1646:207–18. https://doi.org/10.1016/j.brainres.2016.05.045 PMID:27256401

48. Barber AF, Carnevale V, Klein ML, Eckenhoff RG, Covarrubias M. Modulation of a voltage-gated Na+ channel by sevoflurane involves multiple sites and distinct mechanisms. Proc Natl Acad Sci USA. 2014; 111:6726–31. https://doi.org/10.1073/pnas.1405768111 PMID:24753583

49. Liu B, Gu Y, Xiao H, Lei X, Liang W, Zhang J. Altered metabolomic profiles may be associated with sevoflurane-induced neurotoxicity in neonatal rats. Neurochem Res. 2015; 40:788–99. https://doi.org/10.1007/s11064-015-1529-x PMID:25663300

50. Zheng SQ, An LX, Cheng X, Wang YJ. Sevoflurane causes neuronal apoptosis and adaptability changes of neonatal rats. Acta Anaesthesiol Scand. 2013; 57:1167–74. https://doi.org/10.1111/aas.12163 PMID:23889296

51. Siu MT, Weksberg R. Epigenetics of Autism Spectrum Disorder. Adv Exp Med Biol. 2017; 978:63–90. https://doi.org/10.1007/978-3-319-53889-1_4 PMID:28523541

52. Zhou ZB, Yang XY, Yuan BL, Niu LJ, Zhou X, Huang WQ, Feng X, Zhou LH. Sevoflurane-induced down-regulation of hippocampal oxytocin and arginine vasopressin impairs juvenile social behavioral abilities. J Mol Neurosci. 2015; 56:70–77. https://doi.org/10.1007/s12031-014-0468-3 PMID:25417719

53. Lin D, Liu J, Kramberg L, Ruggiero A, Cottrell J, Kass IS. Early-life single-episode sevoflurane exposure impairs social behavior and cognition later in life. Brain Behav. 2016; 6:e00514. https://doi.org/10.1002/brb3.514 PMID:27688943

54. Lee S, Chung W, Park H, Park H, Yoon S, Park S, Park J, Heo JY, Ju X, Yoon SH, Kim YH, Ko Y. Single and multiple sevoflurane exposures during pregnancy and offspring behavior in mice. Paediatr Anaesth. 2017; 27:742–51. https://doi.org/10.1111/pan.13139 PMID:28497474

55. Zhang L, Xue Z, Liu Q, Liu Y, Xi S, Cheng Y, Li J, Yan J, Shen Y, Xiao C, Xie Z, Qiu Z, Jiang H. Disrupted folate metabolism with anesthesia leads to myelination deficits mediated by epigenetic regulation of ERMN. EBioMedicine. 2019; 43:473–86. https://doi.org/10.1016/j.ebiom.2019.04.048 PMID:31060905

56. Raam T, McAvoy KM, Besnard A, Veenema AH, Sahay A. Hippocampal oxytocin receptors are necessary for discrimination of social stimuli. Nat Commun. 2017; 8:2001. https://doi.org/10.1038/s41467-017-02173-0 PMID:29222469

57. Li X, Wu Z, Zhang Y, Xu Y, Han G, Zhao P. Activation of Autophagy Contributes to Sevoflurane-Induced Neurotoxicity in Fetal Rats. Front Mol Neurosci. 2017; 10:432. https://doi.org/10.3389/fnmol.2017.00432 PMID:29311820

58. Cole PD, Finkelstein Y, Stevenson KE, Blonquist TM, Vijayanathan V, Silverman LB, Neuberg DS, Sallan SE, Robaey P, Waber DP. Polymorphisms in Genes Related to Oxidative Stress Are Associated With Inferior Cognitive Function After Therapy for Childhood Acute Lymphoblastic Leukemia. J Clin Oncol. 2015; 33:2205–11. https://doi.org/10.1200/JCO.2014.59.0273 PMID:25987702

59. Su F, Shu H, Ye Q, Wang Z, Xie C, Yuan B, Zhang Z, Bai F. Brain insulin resistance deteriorates cognition by altering the topological features of brain networks. Neuroimage Clin. 2016; 13:280–87. https://doi.org/10.1016/j.nicl.2016.12.009 PMID:28050343

60. Zhong JY, Magnusson KR, Swarts ME, Clendinen CA, Reynolds NC, Moffat SD. The application of a rodent-based Morris water maze (MWM) protocol to an investigation of age-related differences in human spatial learning. Behav Neurosci. 2017; 131:470–82. https://doi.org/10.1037/bne0000219 PMID:29189018

61. Moy SS, Nadler JJ, Perez A, Barbaro RP, Johns JM, Magnuson TR, Piven J, Crawley JN. Sociability and preference for social novelty in five inbred strains: an approach to assess autistic-like behavior in mice. Genes Brain Behav. 2004; 3:287–302. https://doi.org/10.1111/j.1601-1848.2004.00076.x PMID:15344922

62. Justel N, Psyrdellis M, Pautassi RM. Open-field exposure facilitates consummatory extinction. Neuroreport. 2016; 27:1281–86. https://doi.org/10.1097/WNR.0000000000000693 PMID:27749684

63. Selakovic D, Joksimovic J, Obradovic D, Milovanovic D, Djuric M, Rosic G. The adverse effects of exercise and supraphysiological dose of testosterone-enanthate (TE) on exploratory activity in elevated plus maze (EPM) test - indications for using total exploratory activity (TEA) as a new parameter for ex. Neuro Endocrinol

Lett. 2016; 37:383–88.
PMID:28231683

64. Acevedo MB, Nizhnikov ME, Molina JC, Pautassi RM. Relationship between ethanol-induced activity and anxiolysis in the open field, elevated plus maze, light-dark box, and ethanol intake in adolescent rats. Behav Brain Res. 2014; 265:203–15.
https://doi.org/10.1016/j.bbr.2014.02.032
PMID:24583190

65. Kalueff AV, Stewart AM, Song C, Berridge KC, Graybiel AM, Fentress JC. Neurobiology of rodent self-grooming and its value for translational neuroscience. Nat Rev Neurosci. 2016; 17:45–59.
https://doi.org/10.1038/nrn.2015.8
PMID:26675822

66. van den Boom BJ, Pavlidi P, Wolf CJ, Mooij AH, Willuhn I. Automated classification of self-grooming in mice using open-source software. J Neurosci Methods. 2017; 289:48–56.
https://doi.org/10.1016/j.jneumeth.2017.05.026
PMID:28648717

67. Martin M. Cutadapt removes adapter sequences from high-throughput sequencing reads. EMBnet.journal. 2011; 17:10–12.
https://doi.org/10.14806/ej.17.1.200

68. Dobin A, Davis CA, Schlesinger F, Drenkow J, Zaleski C, Jha S, Batut P, Chaisson M, Gingeras TR. STAR: ultrafast universal RNA-seq aligner. Bioinformatics. 2013; 29:15–21.
https://doi.org/10.1093/bioinformatics/bts635
PMID:23104886

69. Love MI, Huber W, Anders S. Moderated estimation of fold change and dispersion for RNA-seq data with DESeq2. Genome Biol. 2014; 15:550.
https://doi.org/10.1186/s13059-014-0550-8
PMID:25516281

70. Reiner A, Yekutieli D, Benjamini Y. Identifying differentially expressed genes using false discovery rate controlling procedures. Bioinformatics. 2003; 19:368–75.
https://doi.org/10.1093/bioinformatics/btf877
PMID:12584122

71. Kolbe AR, Studer AJ, Cornejo OE, Cousins AB. Insights from transcriptome profiling on the non-photosynthetic and stomatal signaling response of maize carbonic anhydrase mutants to low CO_2. BMC Genomics. 2019; 20:138.
https://doi.org/10.1186/s12864-019-5522-7
PMID:30767781

72. McDonough JE, Kaminski N, Thienpont B, Hogg JC, Vanaudenaerde BM, Wuyts WA. Gene correlation network analysis to identify regulatory factors in idiopathic pulmonary fibrosis. Thorax. 2019; 74:132–40.
https://doi.org/10.1136/thoraxjnl-2018-211929
PMID:30366970

73. Sekii K, Yorimoto S, Okamoto H, Nagao N, Maezawa T, Matsui Y, Yamaguchi K, Furukawa R, Shigenobu S, Kobayashi K. Transcriptomic analysis reveals differences in the regulation of amino acid metabolism in asexual and sexual planarians. Sci Rep. 2019; 9:6132.
https://doi.org/10.1038/s41598-019-42025-z
PMID:30992461

74. Wade AA, Lim K, Catta-Preta R, Nord AS. Common CHD8 Genomic Targets Contrast With Model-Specific Transcriptional Impacts of *CHD8* Haploinsufficiency. Front Mol Neurosci. 2019; 11:481.
https://doi.org/10.3389/fnmol.2018.00481
PMID:30692911

75. Ashburner M, Ball CA, Blake JA, Botstein D, Butler H, Cherry JM, Davis AP, Dolinski K, Dwight SS, Eppig JT, Harris MA, Hill DP, Issel-Tarver L, et al, and The Gene Ontology Consortium. Gene ontology: tool for the unification of biology. Nat Genet. 2000; 25:25–29.
https://doi.org/10.1038/75556 PMID:10802651

76. Zhang B, Schmoyer D, Kirov S, Snoddy J. GOTree Machine (GOTM): a web-based platform for interpreting sets of interesting genes using Gene Ontology hierarchies. BMC Bioinformatics. 2004; 5:16.
https://doi.org/10.1186/1471-2105-5-16
PMID:14975175

77. Draghici S, Khatri P, Tarca AL, Amin K, Done A, Voichita C, Georgescu C, Romero R. A systems biology approach for pathway level analysis. Genome Res. 2007; 17:1537–45.
https://doi.org/10.1101/gr.6202607 PMID:17785539

78. Sriroopreddy R, Sajeed R, P R, C S. Differentially expressed gene (DEG) based protein-protein interaction (PPI) network identifies a spectrum of gene interactome, transcriptome and correlated miRNA in nondisjunction Down syndrome. Int J Biol Macromol. 2019; 122:1080–89.
https://doi.org/10.1016/j.ijbiomac.2018.09.056
PMID:30218739

SUPPLEMENTARY MATERIALS

Supplementary Figures

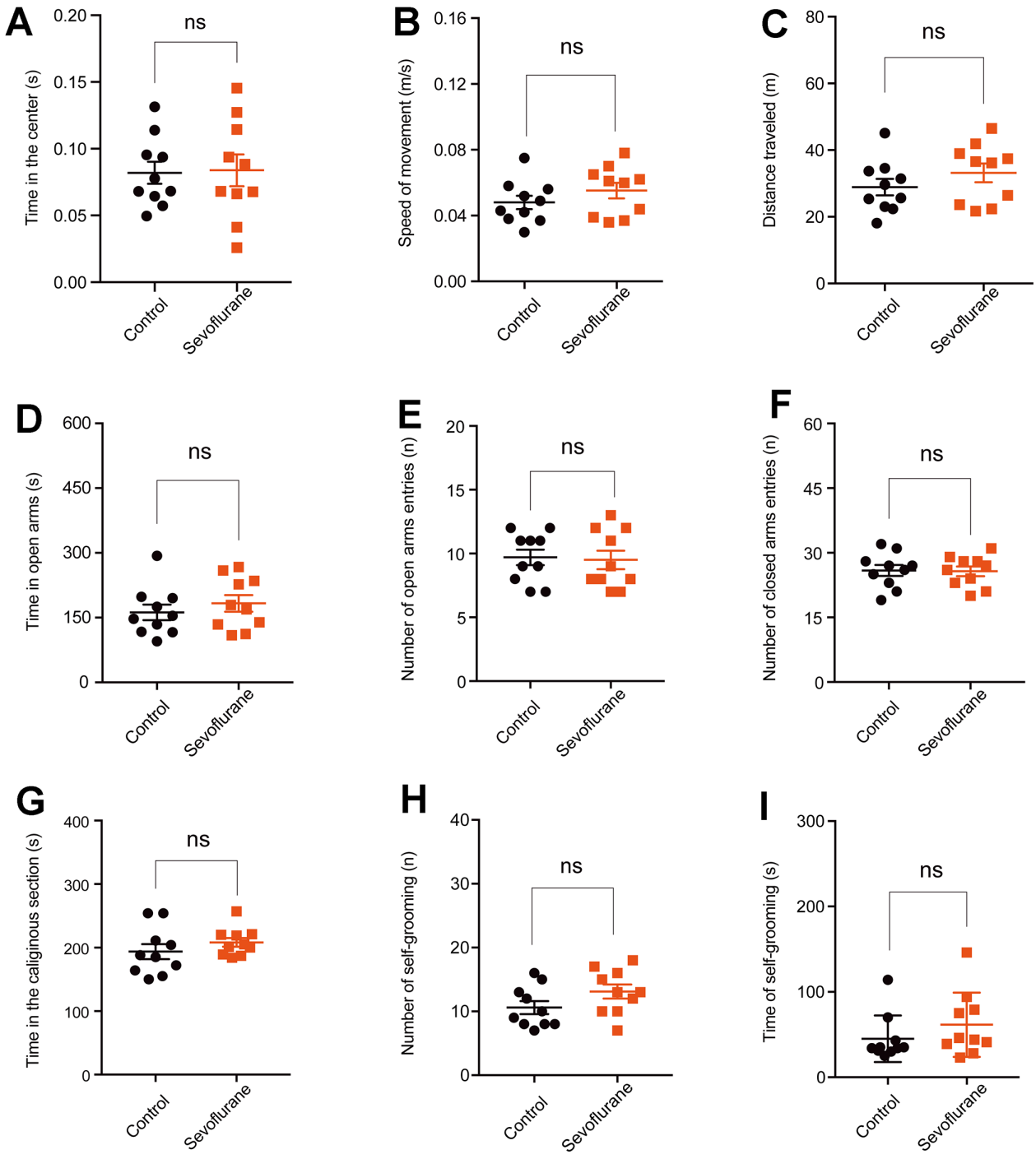

Supplementary Figure 1. Multiple sevoflurane exposures did not induce anxiety-like, depression-like, or stereotyped behaviors. (**A**–**C**) Open field test showing no significant differences in time spent in the center, speed of movement, or distance traveled. (**D**–**F**) Elevated plus maze test showing no significant differences in time of exploring open arms, numbers of open arms entries, or numbers of closed arms entries. (**G**) Light-dark box test showing no significant difference in time spent in the caliginous section. (**H**, **I**) Self-grooming test showing no significant differences in numbers and time of grooming. n = 10.

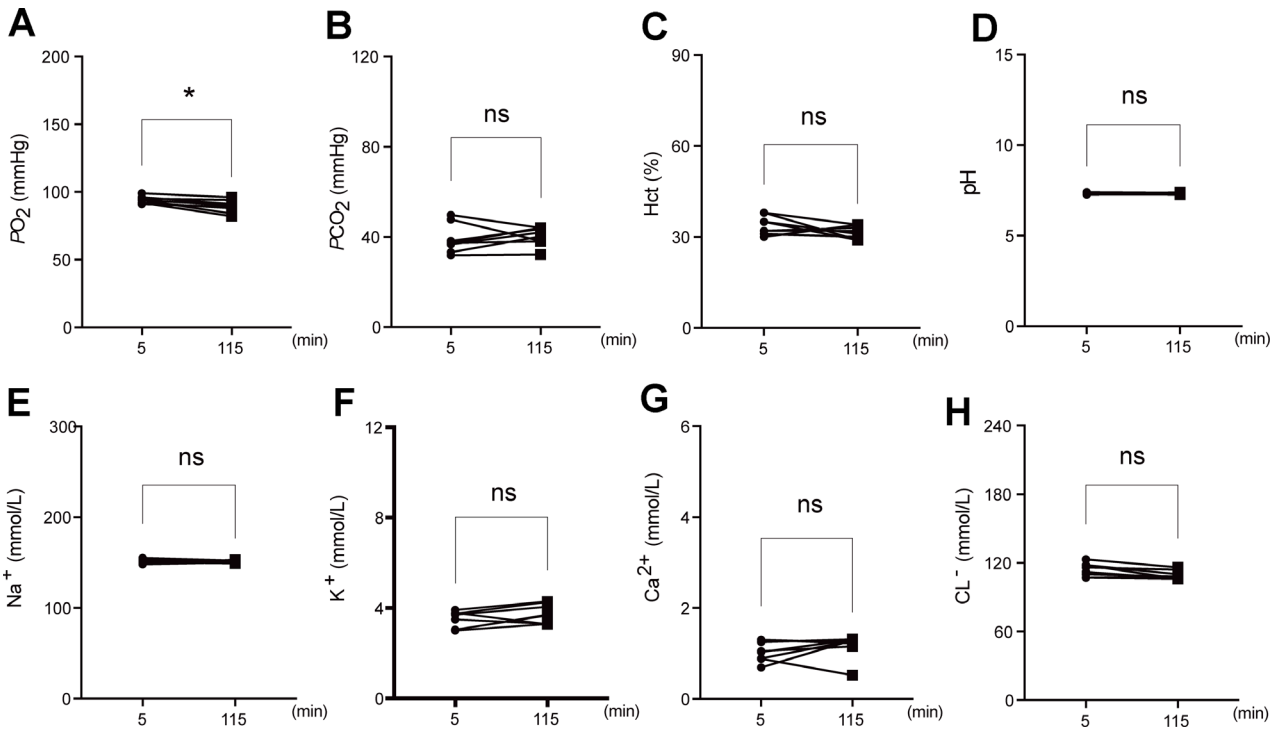

Supplementary Figure 2. Arterial blood gas analysis of mice receiving sevoflurane. Blood samples were taken at 5 min and 115 min during anesthesia on postnatal day 10. (**A**) PO2. (**B**) PCO2. (**C**) Hct. (**D**) pH. (**E**) Na+. (**F**) K+. (**G**) Ca2+. (**H**) Cl-. PO2, arterial oxygen tension; PCO2, arterial carbon dioxide tension; Hct, hematocrit. n = 8. *p < 0.05 for the comparison shown.

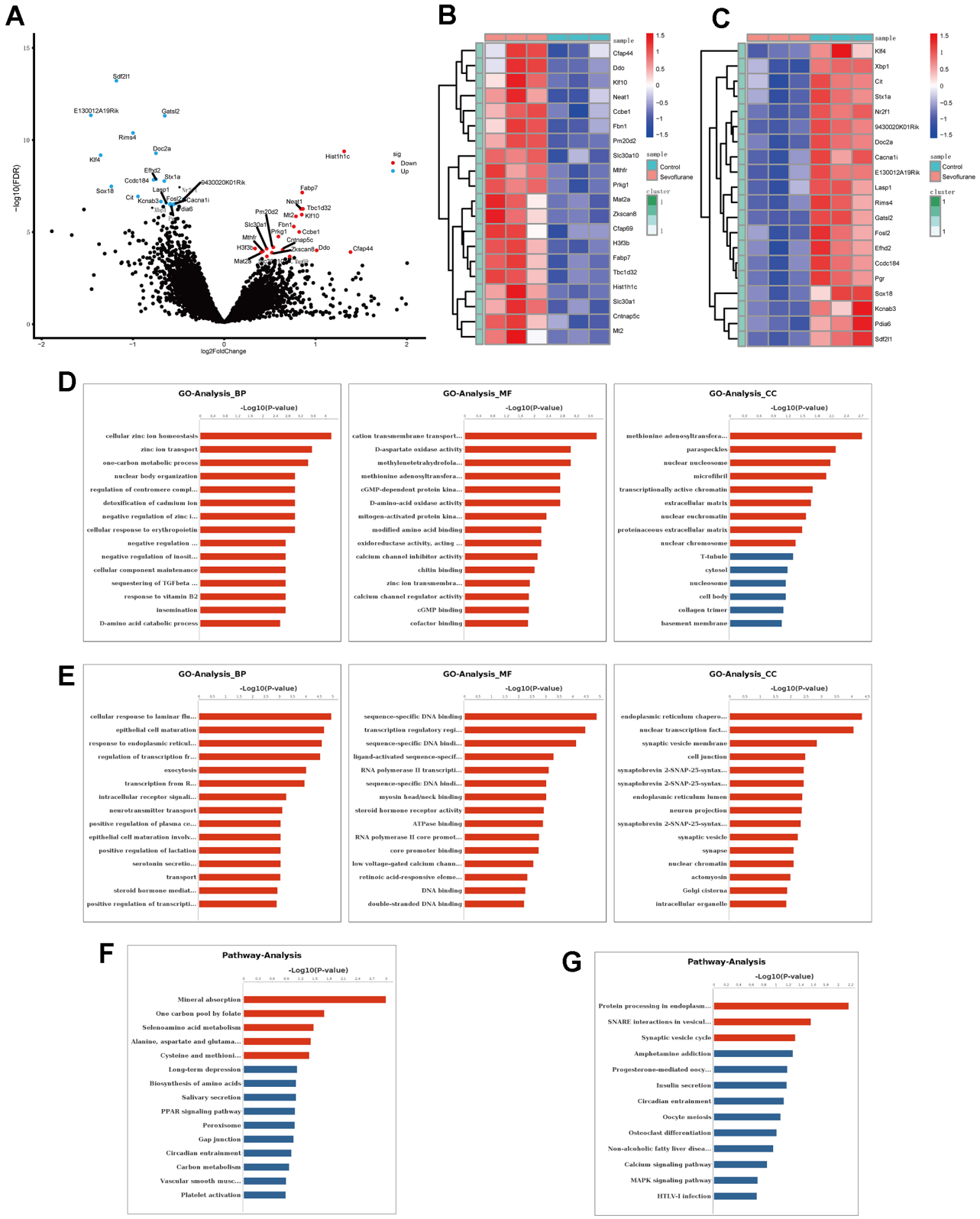

Supplementary Figure 3. Analysis of top 20 up- and down-regulated DEGs. (**A**) Top 20 up- and down-regulated DEGs labeled in volcano plot. (**B**) Heatmap of top 20 up-regulated DEGs. (**C**) Heatmap of top 20 down-regulated DEGs. (**D**) GO terms of BP, MF, and CC based on the top 20 up-regulated DEGs. (**E**) GO terms of BP, MF, and CC based on the top 20 down-regulated DEGs. (**F**) Pathway analysis of top 20 up-regulated DEGs. (**G**) Pathway analysis of top 20 down-regulated DEGs. BP, biological process; MF, molecular function; CC, cellular component. Blue columns indicate terms or pathways without significant difference.

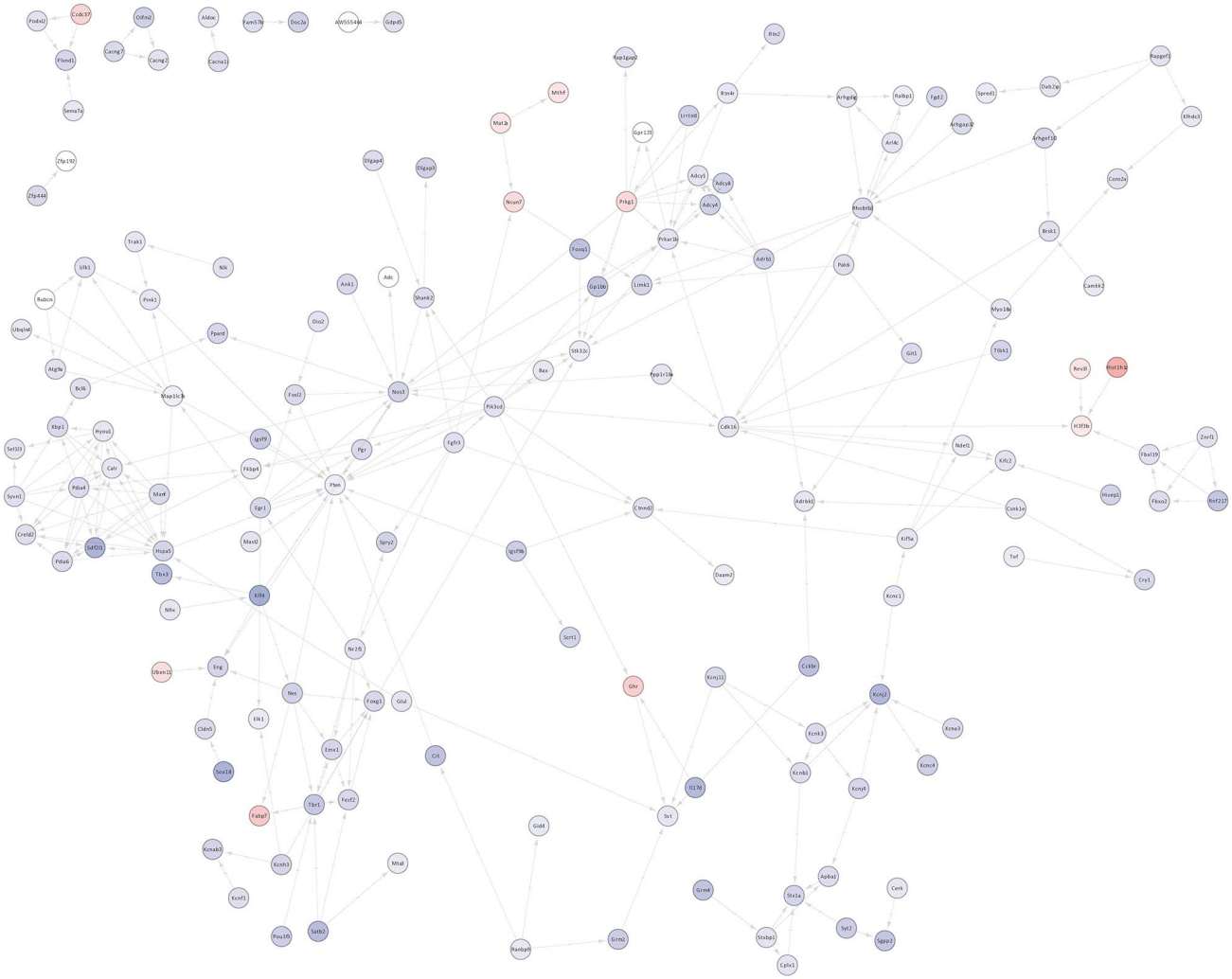

Supplementary Figure 4. PPI network of DEGs in hippocampal tissues between sevoflurane-treated and control mice.

Supplementary Tables

Supplementary Table 1. Primers specific to the top 20 up- and down-regulated DEGs.

Gene	Sequence (5′-3′)	Gene	Sequence (5′-3′)
Up-regulated		Down-regulated	
Hist1h1c-F	AAACTCAACAAGAAGGCGGC	Sdf2l1-F	GCTGCACTCACACGACATCA
Hist1h1c-R	CTTTAGACGCGCTCTTGACC	Sdf2l1-1R	TCCTGGTTGTTGGATAGCGG
Fabp7-F	TGATCCGGACACAATGCACA	E130012A19Rik-1F	TCCTCAGGACTCTCCGACC
Fabp7-R	CCATCCAACCGAACCACAGA	E130012A19Rik-1R	GCGGTTGAAATGTTCCTGGC
Neat1-F	CCTGCTGTCTGCTGGCACTTG	Gatsl2-F	AGACCCCTGAGGACTACACC
Neat1-R	CGTCTCCATCAACTGCTGCTCTG	Gatsl2-R	ACACGGAGATGTTCTGGTCG
Tbc1d32-F	TGCTTCTCACCGAAAACCCAT	Rims4-F	GATGAGGACGCAGCAGACAG
Tbc1d32-R	AAGCAAGCTCATTTTCTGCACC	Rims4-R	CTCCTGCAAGCCAATCTCCA
Klf10-F	CTCAACTTCGGCGCTTCTCT	Doc2a-F	ATGAGGACAAGCTGAGCCAC
Klf10-R	CTCTGCTCAGCTTTGTCCCA	Doc2a-R	CCGCAGACATTGAAGAGGGT
Mt2-F	CGCCTGCAAATGCAAACAATG	Klf4-F	TACCCCTACACTGAGTCCCG
Mt2-R	TCGGAAGCCTCTTTGCAGAT	Klf4-R	GGAAAGGAGGGTAGTTGGGC
Fbn1-F	GTGCAACTGGAAACGGGAAC	Efhd2-F	ACCCCTACACCGAGTTCAAG
Fbn1-R	GCGGGCAAATGCATCTGTAG	Efhd2-R	TCAGGTCGATGAAGCCATCC
Ccbe1-F	ACACGTGGACCTACCGAGAG	Ccdc184-F	ACGGCGGTATGAAGGAACTG
Ccbe1-R	CGCCCGAAGACTTCAGACAT	Ccdc184-R	ACAGAACCTGGATGTGCGAG
Prkg1-F	GGACGCAGAAGCAAAAGCAA	Stx1a-1F	ACCCCGATGAGAGCATTGAG
Prkg1-R	ACTCGTCCGAAACCTCCAAC	Stx1a-1R	TTTGCAGCGTTCTCGGTAGT
Pm20d2-F	CCGAGCACGATGTGACTGT	Sox18-1F	CCTTCTTCCCACCGCCTTT
Pm20d2-R	GGGCGCACGGAAGTAATAGA	Sox18-1R	GGTGGTGACAGAGGATTGGG
H3f3b-F	AAGAAGCCTCACCGCTACAG	Nr2f1-F	AGCGTCCGCAGGAACTTAAC
H3f3b-R	GTGACTCTCTTGGCGTGGAT	Nr2f1-R	TTCTTCCTCGCTGAACCGC
Slc30a1-F	TGGAAGCGGAAGACAACAGG	Cit-F	TTCCTGACGGGGACGTATCT
Slc30a1-R	AGACCAAGGCATTCACGACC	Cit-R	GTCATCGCCCTCCAGTTTCA
Cntnap5c-F	AGATTTACTCAGGCAATGTCACCT	9430020K01Rik-F	GAAGGGGGAGTCCACAACAG
Cntnap5c-R	GGGGGTACCAGTCAACAGC	9430020K01Rik-R	TCTAGTTCCCTGGAGAGCCC
Ddo isoform 1-F	ACAGTGTGTATTGCGGTCGT	Kcnab3-F	ATGCAGGTGTCTATCGCGTG
Ddo isoform 1-R	GTACCGGGGTATCTGCACAC	Kcnab3-R	CCAGGTACCAAGGCCAAGAC
Mthfr isoform a F	CCAGCTGGGCACTGTTATCC	Lasp1-F	CCCAAGCAGTCCTTCACCAT
Mthfr isoform a R	AGTCCATTCTGCGCCTCATC	Lasp1-R	CCACCACGCTGAAACCTTTG
Cfap44-F	TAAGAGCAGCAGCAAGCAGT	Cacna1i-F	GGCTGGACAGCGTCTCTTTA
Cfap44-R	CATAATCTCCAGCTCCGCGT	Cacna1i-R	CTCACCCTTGCTCTCCTTGG
Mat2a-F	AGCTGCTTATGCTGCTCGTT	Fosl2-F	CGGGAACTTTGACACCTCGT
Mat2a-R	TCAGATCCAGATCCCTGACAA	Fosl2-R	GGTGATGGCGTTGATTGTGG
Zkscan8-F	CACTGCAGGGTTCCAGACTT	Pdia6-F	CGTACTGCCTCACATCCTGG
Zkscan8-R	TGGCTGGATTCCGGGAGATA	Pdia6-R	GGTACCCGAACCCTCCAATC
Cfap69-F	GGATGGGGAGATGCAGGGTA	Xbp1-F	CTGAGTCCGCAGCAGGTG
Cfap69-R	GGTTCTACAAAACAGGGCTGC	Xbp1-R	AGGGAGGCTGGTAAGGAACT
Scl30a10-F	CTGCTCTCGGACTCGTTCAA	Pgr1-F	ATCTGGCTGTCACTATGGCG
Scl30a10-R	GCCTCCACGAAGATGGTGAA	Pgr1-R	TGCCAGCCTGACAACACTTT

Supplementary Table 2. All up-regulated DEGs.

AccID	log2FC	Pvalue	Style	AX3HiP1	AX3HiP6	AX3HiP7	C1HiP	C2HiP	C3HiP
Hist1h1c	1.31267581	5.32E-10	up	210	312	310	117	104	93
Fabp7	0.85361146	9.19E-08	up	510	585	626	287	348	263
Neat1	0.83695367	6.96E-07	up	2066	2703	3017	1280	1266	1470
Tbc1d32	0.86251088	7.10E-07	up	334	349	397	176	215	168
Klf10	0.84394199	1.46E-06	up	355	541	655	292	258	246
Mt2	0.79661629	1.74E-06	up	1721	2239	1968	1144	1201	913
Fbn1	0.75822236	6.25E-06	up	347	473	629	261	262	261
Ccbe1	0.81554074	1.23E-05	up	547	680	968	428	309	398
Prkg1	0.59114627	2.20E-05	up	351	358	508	279	248	223
Pm20d2	0.53770463	9.04E-05	up	334	399	545	283	289	242
H3f3b	0.3420804	0.00010199	up	3285	3577	4474	2977	2899	2479
Slc30a1	0.45620874	0.00010528	up	659	805	1034	589	632	473
Cntnap5c	0.63716696	0.00011373	up	335	377	429	277	222	192
Ddo	1.02095372	0.00013425	up	106	193	259	84	83	82
Mthfr	0.41618347	0.00014103	up	879	847	1227	754	695	608
Cfap44	1.38749371	0.00016006	up	233	474	629	91	136	218
Mat2a	0.40471043	0.00017422	up	3246	3280	3948	2675	2721	2074
Zkscan8	0.52475543	0.00017509	up	575	553	673	427	427	328
Cfap69	0.72324972	0.00026348	up	349	370	376	187	241	199
Slc30a10	0.47424661	0.00028382	up	475	495	709	372	436	315
Nphp3	0.67949682	0.00029212	up	294	270	318	181	203	139
Ghr	0.76690226	0.00032131	up	156	214	288	119	111	123
Zfp110	0.71562975	0.0003606	up	239	315	373	164	166	189
Rev3l	0.41260455	0.00036542	up	1385	1376	1726	1142	1045	969
Ccdc37	0.66879606	0.00038	up	168	184	270	115	129	116
Nsun7	0.55639805	0.00045858	up	308	307	381	226	241	171
Traf3ip2	0.70853818	0.00048953	up	295	242	292	181	169	133
Ubxn11	0.53699635	0.00052979	up	257	327	431	224	225	197
Lactb2	0.68114467	0.00059208	up	240	243	257	146	153	137
Col6a4	2.00241304	0.00062403	up	34	188	251	46	14	42
Slc22a4	0.65031318	0.00063502	up	150	160	230	119	116	85
Dsp	0.49510796	0.00064136	up	580	692	946	602	460	399
Adamts3	0.40837859	0.0006738	up	548	564	813	465	458	418
Gm15446	0.89449855	0.00068508	up	177	154	152	86	82	80
A430105I19Rik	0.55366746	0.00071236	up	216	221	306	162	164	144
Vwa3a	0.96074599	0.00079566	up	209	400	422	149	132	198
Zdhhc20	0.3640428	0.00080315	up	1019	1053	1309	893	852	718
Zfp941	0.60698307	0.00080663	up	346	448	495	230	305	253
Xlr3b	1.51243311	0.00084254	up	205	114	107	27	76	44
Kctd4	0.45136281	0.00091241	up	1069	1161	1235	846	833	716
Col25a1	0.54664464	0.0009775	up	1535	1889	3386	1367	1475	1341
Vprbp	0.37143641	0.00100464	up	689	757	935	632	605	487
Dcc	0.48492321	0.00101956	up	881	747	1284	769	655	509
Shtn1	0.4176569	0.00112328	up	732	812	1026	643	567	576
Tex9	0.73468468	0.00115775	up	131	206	214	109	103	96
Zkscan16	0.47956129	0.00116363	up	920	778	1004	679	645	511
A730017C20Rik	0.43986246	0.00122696	up	769	842	1029	620	737	476
Dbi	0.53083746	0.00125356	up	1778	2588	2876	1467	1537	1610
Glb1l	0.60406251	0.00127143	up	278	237	300	175	189	143

Please browse Full Text version to see the data of Supplementary Tables 3–9.

Supplementary Table 3. All down-regulated DEGs.

Supplementary Table 4. All GO terms of biological process associated with up-regulated DEGs.

Supplementary Table 5. All GO terms of biological process associated with down-regulated DEGs.

Supplementary Table 6. All GO terms of cellular component associated with up-regulated DEGs.

Supplementary Table 7. All GO terms of cellular component associated with down-regulated DEGs.

Supplementary Table 8. All GO terms of molecular function associated with up-regulated DEGs.

Supplementary Table 9. All GO terms of molecular function associated with down-regulated DEGs.

Supplementary Table 10. All involved GO terms of biological process in GO-tree analysis.

GOID	GOTerm	Style	2GOID	2GOTerm	2Style	Relation
GO:0000122	negative regulation of transcription from RNA polymerase II promoter	down	GO:0006357	regulation of transcription from RNA polymerase II promoter	down	is_a
GO:0000122	negative regulation of transcription from RNA polymerase II promoter	down	GO:0006366	transcription from RNA polymerase II promoter	down	negatively_ regulates
GO:0000422	mitochondrion degradation	down	GO:0006914	autophagy	down	is_a
GO:0006171	cAMP biosynthetic process	down	GO:0009190	cyclic nucleotide biosynthetic process	down	is_a
GO:0006355	regulation of transcription, DNA-templated	down	GO:0006351	transcription, DNA-templated	down	regulates
GO:0006357	regulation of transcription from RNA polymerase II promoter	down	GO:0006355	regulation of transcription, DNA-templated	down	is_a
GO:0006357	regulation of transcription from RNA polymerase II promoter	down	GO:0006366	transcription from RNA polymerase II promoter	down	regulates
GO:0006366	transcription from RNA polymerase II promoter	down	GO:0006351	transcription, DNA-templated	down	is_a
GO:0006468	protein phosphorylation	down	GO:0016310	phosphorylation	down	is_a
GO:0006811	ion transport	down	GO:0006810	transport	down	is_a
GO:0006836	neurotransmitter transport	down	GO:0006810	transport	down	is_a
GO:0007269	neurotransmitter secretion	down	GO:0006836	neurotransmitter transport	down	is_a
GO:0007416	synapse assembly	down	GO:0007399	nervous system development	down	part_of
GO:0010107	potassium ion import	down	GO:0006813	potassium ion transport	down	is_a
GO:0010506	regulation of autophagy	down	GO:0006914	autophagy	down	regulates
GO:0014047	glutamate secretion	down	GO:0007269	neurotransmitter secretion	down	is_a
GO:0016358	dendrite development	down	GO:0031175	neuron projection development	down	part_of

GO:0018105	peptidyl-serine phosphorylation	down	GO:0006468	protein phosphorylation	down	is_a
GO:0018107	peptidyl-threonine phosphorylation	down	GO:0006468	protein phosphorylation	down	is_a
GO:0033563	dorsal/ventral axon guidance	up	GO:0007411	axon guidance	down	is_a
GO:0035212	cell competition in a multicellular organism	up	GO:0007275	multicellular organismal development	down	part_of
GO:0042977	activation of JAK2 kinase activity	up	GO:0042976	activation of Janus kinase activity	up	is_a
GO:0045893	positive regulation of transcription, DNA-templated	down	GO:0006351	transcription, DNA-templated	down	positively_regulates
GO:0045893	positive regulation of transcription, DNA-templated	down	GO:0006355	regulation of transcription, DNA-templated	down	is_a
GO:0046929	negative regulation of neurotransmitter secretion	up	GO:0007269	neurotransmitter secretion	down	negatively_regulates
GO:0048662	negative regulation of smooth muscle cell proliferation	down	GO:0008285	negative regulation of cell proliferation	down	is_a
GO:0050680	negative regulation of epithelial cell proliferation	down	GO:0008285	negative regulation of cell proliferation	down	is_a
GO:0060074	synapse maturation	down	GO:0007399	nervous system development	down	part_of

Supplementary Table 11. All KEGG pathways associated with up-regulated DEGs.

PathwayID	PathwayTerm	DifGene	AllDifGene	GeneInPathway	AllGene	P-Value	FDR	Enrichment	(-log10P)
PATH:04978	Mineral absorption	2	15	46	7456	0.003715	0.126321	21.61159	2.430003
PATH:03320	PPAR signaling pathway	2	15	81	7456	0.011168	0.189854	12.27325	1.95203
PATH:00670	One carbon pool by folate	1	15	19	7456	0.037585	0.333358	26.1614	1.424991
PATH:00450	Selenoamino acid metabolism	1	15	32	7456	0.062536	0.333358	15.53333	1.203869
PATH:00250	Alanine, aspartate and glutamate metabolism	1	15	37	7456	0.071971	0.333358	13.43423	1.142842
PATH:00270	Cysteine and methionine metabolism	1	15	40	7456	0.077589	0.333358	12.42667	1.110198
PATH:03460	Fanconi anemia pathway	1	15	51	7456	0.09792	0.333358	9.746405	1.009131
PATH:05210	Colorectal cancer	1	15	64	7456	0.121407	0.333358	7.766667	0.915757
PATH:04730	Long-term depression	1	15	73	7456	0.137331	0.333358	6.809132	0.86223
PATH:05412	Arrhythmogenic right ventricular cardiomyopathy	1	15	74	7456	0.139084	0.333358	6.717117	0.856723

	(ARVC)								
PATH:04970	Salivary secretion	1	15	77	7456	0.144322	0.333358	6.455411	0.840667
PATH:01230	Biosynthesis of amino acids	1	15	77	7456	0.144322	0.333358	6.455411	0.840667
PATH:04151	PI3K-Akt signaling pathway	2	15	346	7456	0.15169	0.333358	2.873218	0.819042
PATH:04146	Peroxisome	1	15	82	7456	0.152986	0.333358	6.061789	0.815347
PATH:04540	Gap junction	1	15	87	7456	0.161569	0.333358	5.71341	0.791643
PATH:04974	Protein digestion and absorption	1	15	89	7456	0.164979	0.333358	5.585019	0.782572
PATH:04512	ECM-receptor interaction	1	15	90	7456	0.166679	0.333358	5.522963	0.778119
PATH:04713	Circadian entrainment	1	15	97	7456	0.17849	0.337148	5.124399	0.748386
PATH:01200	Carbon metabolism	1	15	109	7456	0.198375	0.350059	4.560245	0.702513
PATH:04270	Vascular smooth muscle contraction	1	15	128	7456	0.228943	0.350059	3.883333	0.640273
PATH:04611	Platelet activation	1	15	130	7456	0.232097	0.350059	3.82359	0.634331
PATH:04722	Neurotrophin signaling pathway	1	15	133	7456	0.236805	0.350059	3.737343	0.62561
PATH:04360	Axon guidance	1	15	133	7456	0.236805	0.350059	3.737343	0.62561
PATH:05322	Systemic lupus erythematosus	1	15	144	7456	0.253837	0.359603	3.451852	0.595445
PATH:04630	Jak-STAT signaling pathway	1	15	155	7456	0.270514	0.3679	3.206882	0.56781
PATH:04022	cGMP-PKG signaling pathway	1	15	170	7456	0.292696	0.377713	2.923922	0.533583
PATH:05202	Transcriptional misregulation in cancer	1	15	175	7456	0.299949	0.377713	2.840381	0.522953
PATH:05034	Alcoholism	1	15	195	7456	0.328272	0.398616	2.54906	0.483766
PATH:04510	Focal adhesion	1	15	207	7456	0.344748	0.404188	2.401288	0.462498
PATH:04060	Cytokine-cytokine receptor interaction	1	15	260	7456	0.413109	0.466947	1.911795	0.383935
PATH:01100	Metabolic pathways	3	15	1188	7456	0.436412	0.466947	1.255219	0.360103
PATH:04080	Neuroactive ligand-receptor interaction	1	15	282	7456	0.43948	0.466947	1.762648	0.357061
PATH:05200	Pathways in cancer	1	15	325	7456	0.48786	0.502643	1.529436	0.311705
PATH:04740	Olfactory transduction	1	15	1067	7456	0.901626	0.901626	0.465854	0.044974

Please browse Full Text version to see the data of Supplementary Table 12.

Supplementary Table 12. All KEGG pathways associated with down-regulated DEGs.

Supplementary Table 13. All involved KEGG pathways in pathway network analysis.

PathID	PathTerm	Style	2PathID	2PathTerm	2Style
PATH:04015	Rap1 signaling pathway	down	PATH:04020	Calcium signaling pathway	down
PATH:04114	Oocyte meiosis	down	PATH:04914	Progesterone-mediated oocyte maturation	down
PATH:04141	Protein processing in endoplasmic reticulum	down	PATH:05020	Prion diseases	down
PATH:04261	Adrenergic signaling in cardiomyocytes	down	PATH:04020	Calcium signaling pathway	down
PATH:04540	Gap junction	down	PATH:04020	Calcium signaling pathway	down
PATH:04710	Circadian rhythm	down	PATH:04713	Circadian entrainment	down
PATH:04713	Circadian entrainment	down	PATH:04710	Circadian rhythm	down
PATH:04721	Synaptic vesicle cycle	down	PATH:04724	Glutamatergic synapse	down
PATH:04721	Synaptic vesicle cycle	down	PATH:04725	Cholinergic synapse	down
PATH:04721	Synaptic vesicle cycle	down	PATH:04727	GABAergic synapse	down
PATH:04723	Retrograde endocannabinoid signaling	down	PATH:04721	Synaptic vesicle cycle	down
PATH:04723	Retrograde endocannabinoid signaling	down	PATH:04020	Calcium signaling pathway	down
PATH:04723	Retrograde endocannabinoid signaling	down	PATH:04724	Glutamatergic synapse	down
PATH:04723	Retrograde endocannabinoid signaling	down	PATH:04727	GABAergic synapse	down
PATH:04724	Glutamatergic synapse	down	PATH:04721	Synaptic vesicle cycle	down
PATH:04724	Glutamatergic synapse	down	PATH:04020	Calcium signaling pathway	down
PATH:04725	Cholinergic synapse	down	PATH:04721	Synaptic vesicle cycle	down
PATH:04725	Cholinergic synapse	down	PATH:04020	Calcium signaling pathway	down
PATH:04727	GABAergic synapse	down	PATH:04721	Synaptic vesicle cycle	down
PATH:04742	Taste transduction	down	PATH:04020	Calcium signaling pathway	down
PATH:04911	Insulin secretion	down	PATH:05211	Renal cell carcinoma	down
PATH:04911	Insulin secretion	down	PATH:04020	Calcium signaling pathway	down
PATH:04912	GnRH signaling pathway	down	PATH:04020	Calcium signaling pathway	down
PATH:04913	Ovarian steroidogenesis	down	PATH:04912	GnRH signaling pathway	down
PATH:04915	Estrogen signaling pathway	down	PATH:04020	Calcium signaling pathway	down
PATH:04915	Estrogen signaling pathway	down	PATH:04913	Ovarian steroidogenesis	down
PATH:04915	Estrogen signaling pathway	down	PATH:04727	GABAergic synapse	down
PATH:04918	Thyroid hormone synthesis	down	PATH:04020	Calcium signaling pathway	down
PATH:04970	Salivary secretion	down	PATH:04020	Calcium signaling pathway	down
PATH:04971	Gastric acid secretion	down	PATH:04020	Calcium signaling pathway	down
PATH:05032	Morphine addiction	down	PATH:04727	GABAergic synapse	down
PATH:05166	HTLV-I infection	down	PATH:04115	p53 signaling pathway	down
PATH:05213	Endometrial cancer	down	PATH:04115	p53 signaling pathway	down
PATH:05221	Acute myeloid leukemia	down	PATH:04150	mTOR signaling pathway	down